we noted an accumulation of Tet$^+$CD8$^+$ T cells that had divided once and then stopped further proliferation. This proliferation-aborted population increased in ratio, whereas the population under multiple cell divisions reciprocally decreased, in proportion to the number of added T_{reg} cells. The proliferation-aborted cells had significantly lower tetramer staining intensity than the cells that had vigorously proliferated in the absence of T_{reg} cells (peak a versus b in Fig. 1A, Fig. 1B, and fig. S1). The staining intensity of T cell receptor-αβ (TCR-αβ) chains was equivalent in both populations, which indicated that the lower tetramer staining intensity was not due to down-modulation of TCR but to lower TCR affinity for the Melan-A peptide, as supported by significantly lower ratios of tetramer versus TCR-αβ staining intensities (Fig. 1C). Functionally, they produced reduced levels of cytokines such as interferon-γ (IFN-γ), tumor necrosis factor-α (TNF-α), and interleukin 2 (IL-2) (Fig. 1, D and E), despite the addition of exogenous IL-2 to maintain cultured T cells. Furthermore, upon secondary stimulation, they remained hypoproliferative and produced very low amounts of cytokines (fig. S2). Thus, antigenic stimulation under T_{reg} cell–mediated suppression allows responder T cells with relatively low affinity TCRs for a self-antigen to divide once but prevents their further proliferation, which drives them into a profoundly and stably hypoproliferative and cytokine-hypoproducing state, which can be immunologically defined as "anergy" (*10–13*).

In contrast with anti–Melan-A responses, CD8$^+$ T cells from the same donor, who had detectable serum anticytomegalovirus (CMV) immunoglobulin G (IgG) antibody, had CMV peptide–specific T cells with a memory phenotype (fig. S3, A to D). CMV-specific CD8$^+$ T cells, whether they were in a naïve or memory cell fraction, vigorously proliferated and produced inflammatory cytokines even at a high T_{reg}-to-responder T cell ratio, with no significant differences in CMV tetramer staining intensity among CD8$^+$ T cells proliferating in the presence or absence of T_{reg} cells (fig. S3, E to H). However, high numbers of T_{reg} cells completely inhibited the proliferation of polyclonally activated naïve CD8$^+$ T cells without allowing a single cell division (fig. S4). The nondividing CD8$^+$ T cells proliferated as actively as nonsuppressed cells upon restimulation after removal of T_{reg} cells.

Collectively, T_{reg}-cell dosage, the immunological states of responder T cells (e.g., in a naïve or memory state), and their TCR affinity for cognate antigen contribute to T_{reg} cell–mediated induction of anergy. This is an active process and differs from a mere naïve nonproliferative state.

Microarray gene expression analysis revealed that activated or anergic Tet$^+$CD8$^+$ T cells or Tet$^-$CD8$^+$ T cells obtained from T_{reg}-absent or -present cell cultures were substantially different in gene expression profiles (Fig. 2A). As the most striking differences, the transcription of *CTLA4*, encoding the coinhibitory molecule CTLA-4 (*14*), was significantly up-regulated, whereas *BCL2*, encoding the apoptosis-inhibiting molecule B cell lymphoma-2 (BCL-2) (*15*), was down-regulated in anergic CD8$^+$ T cells, as confirmed by quantitative reverse transcription polymerase chain reaction (RT-PCR) (Fig. 2B). There were no significant differences in the expression of *PDCD1* encoding the coinhibitory molecule PD-1; the genes encoding the anergy-related molecules GRAIL, CBL-B, and EGR-2 (*16–19*); BAT3, TBX21, and EOMES, putative markers for exhausted CD8$^+$ T cells (*20*, *21*); and p27KIP1, a cyclin-dependent kinase inhibitor. Anergic CD8$^+$ T cells did not express FoxP3 (Fig. 2B and fig. S5A). The majority (>90%) of anergic CD8$^+$ T cells expressed both CTLA-4 and the chemokine receptor CCR7, which differed from the phenotype of activated or naïve CD8$^+$ T cells (Fig. 2, C and D, and fig. S5, B to D) (*22*, *23*). Functionally, during secondary stimulation of anergic Tet$^+$CD8$^+$ T cells with Melan-A peptide–pulsed APCs after removal of T_{reg} cells, antibody blockade of CTLA-4 and PD-1 at doses enhancing cytokine production by activated conventional T cells failed to rescue proliferation resistance or cytokine hypoproduction of anergic CD8$^+$ T cells (fig. S5E) (*24*). Addition of a high dose of IL-2 induced apoptosis in restimulated Tet$^+$CD8$^+$ T cells rather than abrogating their hyporesponsiveness. Nevertheless, anergic CD8$^+$ T cells were not in the process of immediate apoptosis (fig. S6), despite their lower *BCL2* expression than activated T cells (Fig. 2B). Thus, anergic CD8$^+$ T cells induced by T_{reg} cell–mediated suppression are distinct from activated or naïve T cells in gene and protein expression profiles. They also appear to be different from "exhausted" CD8$^+$ T cells, which develop as PD-1$^+$ hypoproliferative and cytokine-hypoproducing cells

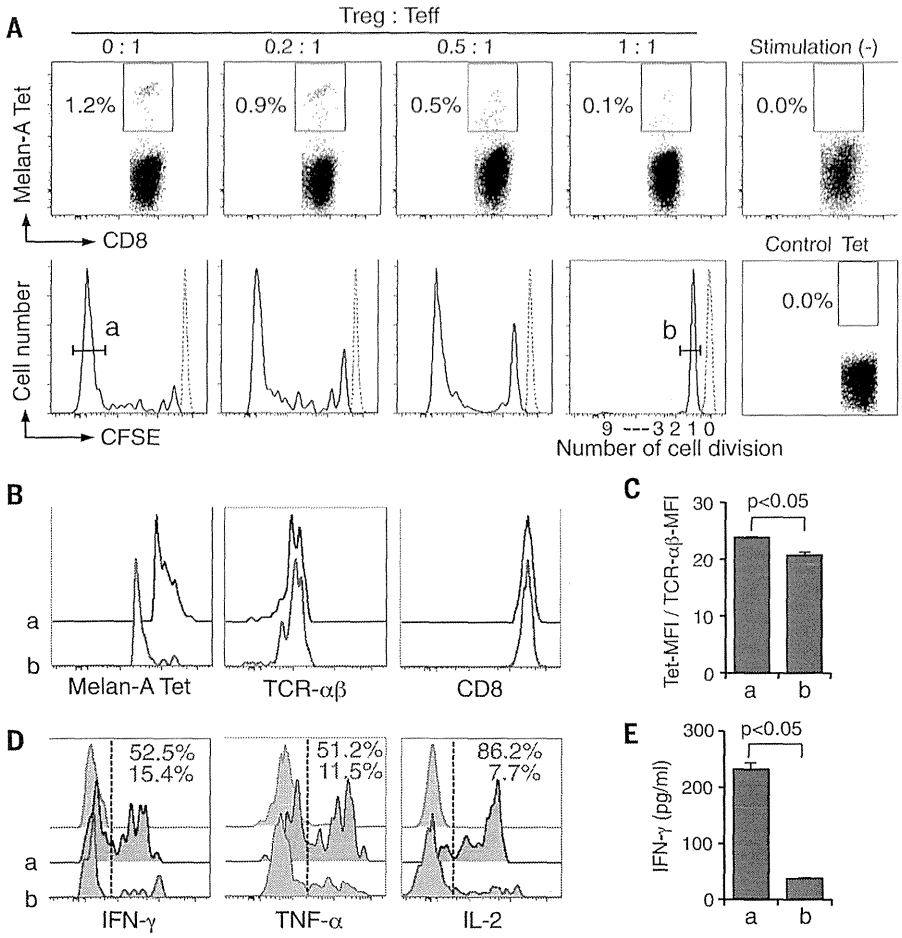

Fig. 1. Natural T_{reg} cells render low-affinity self-reactive CD8$^+$ T cells anergic upon antigen stimulation. (**A**) Melan-A–specific CD8$^+$ T cell induction. CFSE-labeled CD8$^+$ T cells of HLA-A*0201$^+$ healthy individuals were stimulated by T cell–depleted, γ-irradiated, and Melan-A_{26-35} peptide–pulsed APCs with graded numbers of CD25^{high}CD4$^+$ T_{reg} cells for 10 days (*6*). Dotted lines mean Tet$^-$CD8$^+$ cells showing no CFSE dilution. Control tet: NY-ESO-$1_{157-165}$/HLA-A*0201 tetramer. T_{eff} refers to CD8$^+$ effector T cells. (**B**) Tet, TCR-αβ, and CD8 staining of Tet$^+$CD8$^+$ T cells. Results in (A) and (B) are representative of 10 independent experiments. (**C**) Relative tetramer staining intensities, calculated as mean fluorescence intensity (MFI) of Tet/MFI of TCR-αβ staining of Tet$^+$CD8$^+$ T cells (n = 5). (**D** and **E**) Cytokine production of Tet$^+$CD8$^+$ T cells by intracellular staining (D) and enzyme-linked immunosorbent assay (E) (*6*). Representative result of three independent experiments. The labels a and b in (B) to (E) mean the cell accumulations like a or b in (A). Error bars indicate means ± SEM. The significance was assessed by Student's two-tailed paired t test.

in chronic viral infections and in tumor tissues, because exhausted $CD8^+$ T cells are reportedly $CCR7^-$, $CD45RA^-$, and $BAT3^+$, and their exhaustion can be rescued by a PD-1–blocking antibody (*21*, *24*–*26*).

T_{reg} cells suppress the activation and/or proliferation of responder T cells (*27*), at least in part, by down-regulating the expression of the costimulatory molecules CD80 and CD86 on APCs (fig. S7A) (*28*, *29*). To determine whether low expression or down-modulation of CD80 and CD86 on dendritic cells (DCs) was responsible for the induction of antigen-specific anergic $CD8^+$ T cells, we stimulated carboxyfluorescein succinimidyl ester (CFSE)–labeled $CD8^+$ T cells with autologous immature or mature DCs pulsed with Melan-A peptide in the presence of graded amounts of CTLA-4–immunoglobulin (CTLA-4Ig), which blocked CD80 and CD86 (fig. S7B) (*30*). In contrast to the vigorous proliferation of Tet^+CD8^+ T cells cultured with mature DCs, the majority of Tet^+CD8^+ T cells generated with immature DCs, and some with mature DCs with a high dose (100 μg/ml) of CTLA-4Ig, were proliferation-aborted after one cell division (Fig. 3A). The proliferation-aborted T cells (peaks c and d in Fig. 3A) were lower than proliferating T cells in Melan-A tetramer staining intensity (Fig. 3B), and highly expressed CTLA-4 and CCR7 (fig. S7, C and D); they formed a discrete CTLA-4/CCR7 double-positive population (Fig. 3C and fig. S7E). They produced significantly lower amounts of IFN-γ, TNF-α, and IL-2 compared with Tet^+CD8^+ cells, having proliferated in culture with mature DCs (fig. S7F). Similar to peptide stimulation, polyclonal antibody against CD3-specific monoclonal antibody (mAb) stimulation of $CTLA4^-$ naïve $CD8^+$ T cells in the presence of CTLA-4Ig produced cells that were proliferation-aborted after one cell division (fig. S8A). Notably, increasing CTLA-4Ig dose proportionally intensified CTLA-4 expression by the aborted cells, while stably maintaining their high CCR7 expression (fig. S8, A and B). Taken together, antigen presentation with low CD80 and CD86 costimulation is able to drive $CD8^+$ T cells to differentiate into $CTLA\text{-}4^+CCR7^+$ anergic cells. DCs with moderate CD80 and CD86 reduction can concurrently generate both

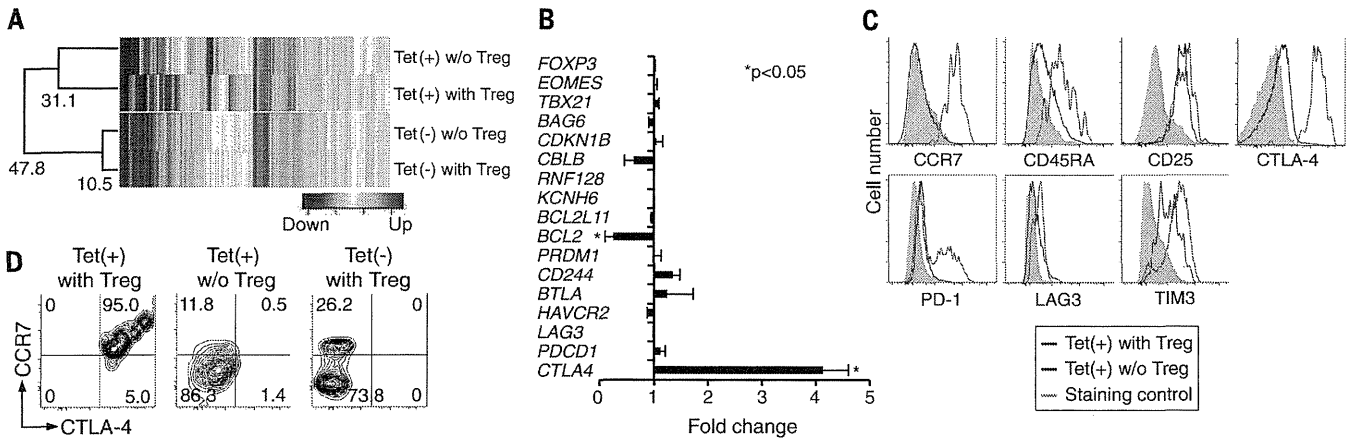

Fig. 2. Distinct phenotype and function of anergic $CD8^+$ T cells produced by T_{reg} cell suppression. (**A**) Global mRNA expression profile. Tet^+CD8^+ T cells induced at $CD8^+$ T cells: T_{reg} cell ratios of 1:0.5 and 1:0 were subjected to microarray analyses. Gene expression reportedly associated with $CD8^+$ T cell function was compared among the indicated four groups and expressed as a heat map. Correlation distances shown were calculated by h-clust (*6*). Representative of two independent experiments. (**B**) mRNA expression measured by quantitative real-time PCR. Fold changes of mRNA level as [Tet(+) with T_{reg}] versus [Tet(+) without T_{reg}] in five independent experiments are shown. Error bars indicate means ± SEM. (**C** and **D**) Expression of cell surface molecules by Tet^+CD8^+ T cells induced at $CD8^+$ T cells: T_{reg} cell ratios, 1:1 and 1:0. Representative histogram staining pattern (C) and contour plot staining pattern of CTLA-4 and CCR7 (D). Data are representative of five independent experiments (n = 10). The significance was assessed by Student's two-tailed paired t test.

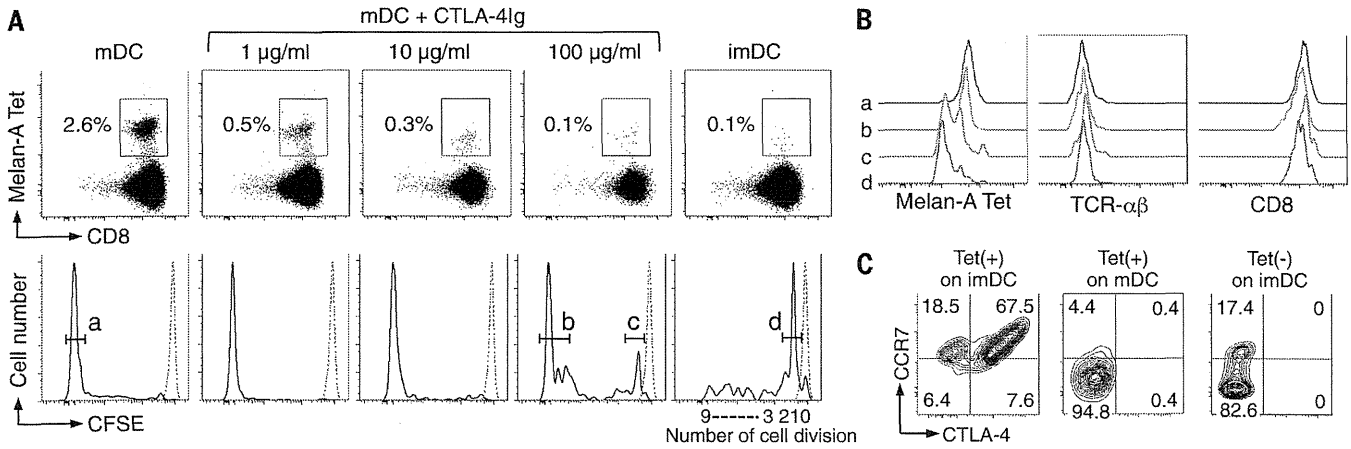

Fig. 3. DC expression of CD80 and CD86 controls the generation of $CTLA\text{-}4^+CCR7^+$ low-affinity anergic self-reactive T cells. (**A**) Melan-A–specific $CD8^+$ T cell induction. CFSE-labeled $CD8^+$ T cells of HLA-A*0201$^+$ healthy individuals were stimulated with γ-irradiated, Melan-$A_{26\text{-}35}$ peptide–pulsed monocyte-derived immature or mature DCs. CTLA-4Ig was added into mature DCs cultures at indicated concentrations (*6*). (**B**) Tet, TCR-αβ, and CD8 staining intensity of Tet^+CD8^+ T cells shown in (A). (**C**) Representative contour plot staining pattern of Tet^+ or Tet^-CD8^+ T cells shown in (A) for CTLA-4 and CCR7. Data in (A) to (C) are representative of five independent experiments.

activated T cells and anergic T cells, in part, depending on TCR affinity.

The above in vitro findings prompted us to ask whether healthy individuals harbored such anergic self-reactive $CD8^+$ T cells. Direct ex vivo staining of $CD8^+$ T cells in PBMCs of healthy donors ($n = 10$) for Melan-A peptide and MHC tetramer, with $CD8^+$ T cells from vitiligo patients ($n = 10$) as a positive control, revealed that a small number of Tet^+CD8^+ T cells were indeed present in healthy individuals and constituted ~0.03% of $CD8^+$ T cells in PBMCs, which contrasted with high percentages (~0.1%) in vitiligo patients (Fig. 4, A and B) (*6*). Two-thirds of the former had a naïve ($CCR7^+CD45RA^+$) phenotype, whereas the majority of the latter had an effector or memory phenotype (Fig. 4C and fig. S9A) (*4*, *5*). The Tet^+CD8^+ T cells from healthy individuals had significantly lower tetramer staining intensity than those from vitiligo patients (Fig. 4, D and E). They expressed CTLA-4 at higher levels than Tet^+CD8^+ T cells from vitiligo patients or Tet^-CD8^+ T cells from healthy individuals, or activated $CD8^+$ T or natural T_{reg} cells (Fig. 4F and fig. S9, B to D), and ~90% of the $Tet^+CD45RA^+CD8^+$ cells were double positive for CTLA-4 and CCR7 (Fig. 4G and fig. S9B). Functionally, Tet^+CD8^+ T cells directly prepared from healthy donors scarcely produced IFN-γ, TNF-α, or IL-2, contrasting with active cytokine production by naïve Tet^-CD8^+ T cells (Fig. 4H) or Melan-A–specific $CD8^+$ T cells from vitiligo patients (*4*, *31*).

To determine further the function of these anergic T cells, we cocultured $CTLA\text{-}4^+$ and $CTLA\text{-}4^-$ fractions of naïve ($CCR7^+CD45RA^+$) $CD8^+$ T cells from healthy individuals and assessed the proliferative activity of Tet^+CD8^+ T cells present in each fraction (Fig. 4I). The $CTLA\text{-}4^+$ fraction, which constituted less than 10% of naïve $CD8^+$ T cells in healthy donors, contained the majority (~95%) of Melan-A Tet^+CD8^+ T cells before stimulation (Fig. 4, I to K). These $CTLA\text{-}4^+Tet^+$ cells were

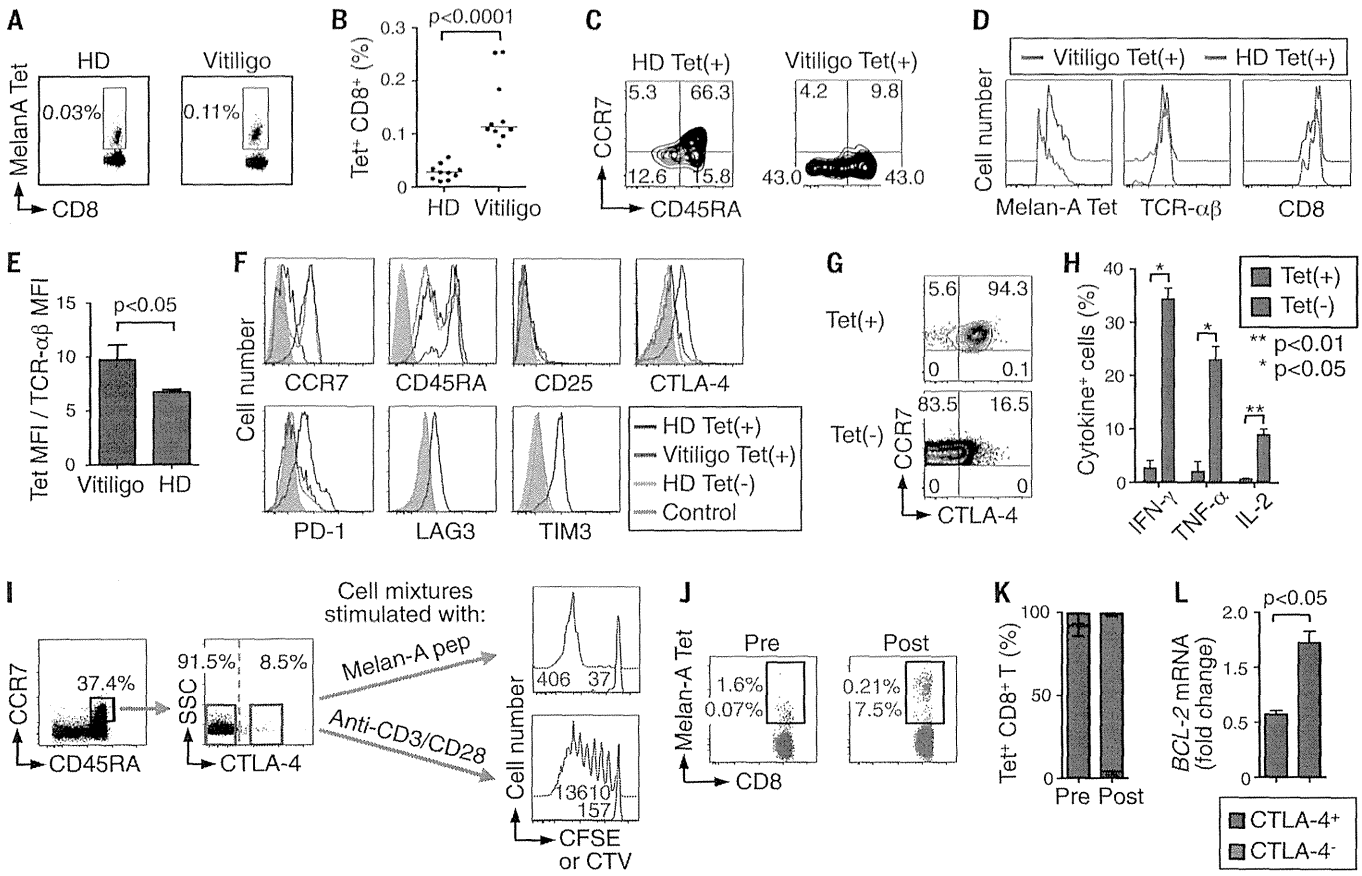

Fig. 4. Detection of low-affinity anergic self-reactive $CTLA\text{-}4^+CCR7^+CD8^+$ T cells in healthy individuals. (**A**) Melan-ATet^+CD8^+ T cells in PBMCs of a healthy donor (HD) and a vitiligo patient. (**B**) Percentages of Tet^+CD8^+ T cells in HDs and vitiligo patients ($n = 10$). (**C**) CCR7 and CD45RA expression by Tet^+CD8^+ T cells in an HD and a vitiligo patient. (**D**) Tet, TCR-αβ, and CD8 staining intensity of Tet^+CD8^+ T cells in an HD and a vitiligo patient. (**E**) Ratios of MFI of tetramer staining to MFI of TCR-αβ staining in Tet^+CD8^+ T cells in HDs and vitiligo patients ($n = 4$ each). (**F**) Expression of cell surface molecules by Tet^+ or Tet^-CD8^+ T cells in a representative HD and a vitiligo patient. (**G**) Representative staining for CTLA-4 and CCR7 of Tet^+ or Tet^- cells in $CD45RA^+CD8^+$ T cells of an HD. Data shown in (A), (C), (D), (F), and (G) are representative of four independent experiments. (**H**) Cytokine production by Tet^+CD8^+ T cells in HDs assessed by intracellular staining with $CCR7^+CD45RA^+Tet^-CD8^+$ T cells as control. Data summarize four independent experiments. (**I**) Proliferation and cytokine production of $CTLA\text{-}4^+$ or $CTLA\text{-}4^-$ naïve $CD8^+$ T cells in HDs. $CCR7^+CD45RA^+CD8^+$ T cells from HD PBMCs were further separated into $CTLA\text{-}4^+$ and $CTLA\text{-}4^-$ cells, labeled with Cell Trace Violet (CTV) or CFSE, respectively, mixed at a 1:1 ratio, stimulated with Melan-$A_{26\text{-}35}$ peptide–pulsed APCs for 10 days (top) or CD3/CD28-specific mAb for 5 days (bottom), and assessed for proliferation by CTV or CFSE dilution (red and blue, respectively) (*6*). Numbers in right two figures represent the numbers of cells in each cell fraction. SSC, side scatter. (**J**) Representative tetramer staining of the cell mixtures before (Pre) and after (Post) Melan-$A_{26\text{-}35}$ peptide stimulation for 10 days. Numbers represent percentages of Tet^+CD8^+ cells in the $CTLA\text{-}4^+$ or $CTLA\text{-}4^-$ fraction (red and blue, respectively). (**K**) Percentages of Tet^+CD8^+ T cells in the $CTLA\text{-}4^+$ (red) or $CTLA\text{-}4^-$ (blue) fraction in the cell mixtures before (Pre) and after (Post) cell culture as shown in (I) and (J). (**L**) *BCL2* mRNA expression of $CTLA\text{-}4^+CCR7^+CD45RA^+Tet^+CD8^+$ and $CTLA\text{-}4^-CCR7^+CD45RA^+Tet^+CD8^+$ T cells measured by quantitative real-time PCR. Data in (I) to (L) are representative of at least three independent experiments. Error bars indicate means ± SEM. The significance was assessed by Student's two-tailed paired *t* test.

hypoproliferative, low in *BCL2* expression, and prone to die upon Melan-A stimulation (Fig. 4, I to L). In contrast, the CTLA-4$^-$ fraction, which initially contained fewer than 5% of total Tet$^+$CD8$^+$ T cells, gave rise to proliferating Tet$^+$CD8$^+$ T cells, which made up ~95% of total Tet$^+$CD8$^+$ T cells after stimulation (Fig. 4, I to K). In addition, polyclonal stimulation of the cell mixtures with CD3-specific and CD28-specific mAb revealed that the CTLA-4$^+$ fraction as a whole was hypoproliferative (Fig. 4I) and cytokine hypoproducing (fig. S9E), in contrast with active proliferation and cytokine production of the CTLA-4$^-$ fraction.

These results collectively indicate that healthy individuals harbor at least two distinct populations of self-reactive CD8$^+$ T cells: one that is functionally anergic and expresses CTLA-4 and CCR7 and another that is CTLA-4$^-$ and naïve in function and phenotype. The latter, especially those with high-affinity TCRs, may become activated and expand upon self-antigen stimulation in the absence or reduction of natural T_{reg} cells, as shown in Fig. 1A.

Thus, anergic self-reactive T cells, which are phenotypically distinct from other T cells, are physiologically present in the immune system. They appear to be generated, at least in part, as a result of T_{reg}-mediated suppression, which can determine cell fate of responder T cells (i.e., activated, anergic, or ignorant) upon antigenic stimulation, depending on the number and suppressive activity of T_{reg} cells, the TCR affinity and differentiation states of responder T cells, and the condition of APCs. This T_{reg}-dependent switching of responder T cell fate can be a key target in controlling autoimmunity and tumor immunity, as illustrated by our analysis of Melan-A-specific immune responses, as well as a variety of other physiological and pathological immune responses.

REFERENCES AND NOTES

1. S. Sakaguchi, *Nat. Immunol.* **6**, 345–352 (2005).
2. P. G. Coulie *et al.*, *J. Exp. Med.* **180**, 35–42 (1994).
3. Y. Kawakami *et al.*, *Proc. Natl. Acad. Sci. U.S.A.* **91**, 6458–6462 (1994).
4. G. S. Ogg, P. Rod Dunbar, P. Romero, J. L. Chen, V. Cerundolo, *J. Exp. Med.* **188**, 1203–1208 (1998).
5. M. J. Pittet *et al.*, *J. Exp. Med.* **190**, 705–716 (1999).
6. Materials and methods are available as supplementary materials on *Science* Online.
7. M. Itoh *et al.*, *J. Immunol.* **162**, 5317–5326 (1999).
8. C. S. Hsieh, H. M. Lee, C. W. Lio, *Nat. Rev. Immunol.* **12**, 157–167 (2012).
9. T. Yamaguchi *et al.*, *Proc. Natl. Acad. Sci. U.S.A.* **110**, E2116–E2125 (2013).
10. M. K. Jenkins, R. H. Schwartz, *J. Exp. Med.* **165**, 302–319 (1987).
11. R. H. Schwartz, *Annu. Rev. Immunol.* **21**, 305–334 (2003).
12. F. Macián, S. H. Im, F. J. García-Cózar, A. Rao, *Curr. Opin. Immunol.* **16**, 209–216 (2004).
13. A. D. Wells, *J. Immunol.* **182**, 7331–7341 (2009).
14. A. H. Sharpe, G. J. Freeman, *Nat. Rev. Immunol.* **2**, 116–126 (2002).
15. P. E. Czabotar, G. Lessene, A. Strasser, J. M. Adams, *Nat. Rev. Mol. Cell Biol.* **15**, 49–63 (2014).
16. N. Anandasabapathy *et al.*, *Immunity* **18**, 535–547 (2003).
17. M. S. Jeon *et al.*, *Immunity* **21**, 167–177 (2004).
18. D. L. Mueller, *Nat. Immunol.* **5**, 883–890 (2004).
19. Y. Zheng, Y. Zha, G. Driessens, F. Locke, T. F. Gajewski, *J. Exp. Med.* **209**, 2157–2163 (2012).
20. M. A. Paley *et al.*, *Science* **338**, 1220–1225 (2012).
21. M. Rangachari *et al.*, *Nat. Med.* **18**, 1394–1400 (2012).
22. F. Sallusto, D. Lenig, R. Förster, M. Lipp, A. Lanzavecchia, *Nature* **401**, 708–712 (1999).
23. M. A. Williams, M. J. Bevan, *Annu. Rev. Immunol.* **25**, 171–192 (2007).
24. D. L. Barber *et al.*, *Nature* **439**, 682–687 (2006).
25. S. D. Blackburn *et al.*, *Nat. Immunol.* **10**, 29–37 (2009).
26. E. J. Wherry, *Nat. Immunol.* **12**, 492–499 (2011).
27. E. M. Shevach, *Immunity* **30**, 636–645 (2009).
28. K. Wing *et al.*, *Science* **322**, 271–275 (2008).
29. O. S. Qureshi *et al.*, *Science* **332**, 600–603 (2011).
30. J. A. Bluestone, E. W. St. Clair, L. A. Turka, *Immunity* **24**, 233–238 (2006).
31. K. S. Lang *et al.*, *J. Invest. Dermatol.* **116**, 891–897 (2001).

ACKNOWLEDGMENTS

We thank Y. Tada, K. Teshima, and Y. Funabiki for technical assistance. The data presented in this paper are tabulated in the main paper and in the supplementary materials. Microarray data are deposited in GSE63129. This study was supported by Grants-in-Aid for Specially Promoted Research (to S.S., no. 20002007) and for Scientific Research (i) (to S.S., no. 26253030) and (ii) (to H.N., no. 23300354 and 26290054) from the Ministry of Education, Culture, Sports, Science, and Technology of Japan; Core Research for Evolutional Science and Technology (CREST) from Japan Science and Technology Agency (to S.S.); Health and Labor Sciences Research Grants, Research on Applying Health Technology (H24-Clinical Cancer Research-general-006 to H.N.) from the Ministry of Health, Labor, and Welfare, Japan, the Cancer Research Institute CLIP grant to H.N. All authors have no competing financial interest.

SUPPLEMENTARY MATERIALS

www.sciencemag.org/content/346/6216/1536/suppl/DC1
Materials and Methods
Supplemental Text
Figs. S1 to S9
References (*32*–*37*)

21 October 2014; accepted 20 November 2014
10.1126/science.aaa1292

RNAi-induced loss of *pat-10* disrupts endocytosis through impairment of the actin cytoskeleton (*12*, *13*, *15*). To assay the role of *pat-10* in endocytosis, we used a secretion and endocytosis reporter designed to actively secrete GFP (ssGFP) from muscle cells into the pseudocoelomic fluid, where it is endocytosed by the coelomocyte cells and degraded (fig. S9A) (*16*). Therefore, the ssGFP reports upon effective muscular secretion and endocytosis by coelomocytes. Fitting the hypothesis that *pat-10* overexpression improves transport and cellular processing through improved subcellular scaffolding, the *pat-10 OE* strain had a decrease in overall ssGFP fluorescence (Fig. 3, E and F). The decrease in ssGFP resulted from improved secretion and uptake, as shown by the absence of fluorescence in the muscle and pseudocoelomic fluid (Fig. 3E). This decrease was not due to an overall decrease in expression of GFP (fig. S9B). Conversely, RNAi of *pat-10* increased overall fluorescence through decreased muscle secretion and coelomocytic endocytosis (Fig. 3, E and G). To fully block coelomocytic uptake and degradation of ssGFP, RNAi of *cup-4*, a ligand-gated ion channel required in endocytosis (*17*), showed an even higher increase in fluorescence (Fig. 3G) and also reduced thermotolerance in the wild type (Fig. 3H). Collectively, these data indicate *pat-10* has an active role in cytoskeletal maintenance, which is critical to cellular transport.

To test for conservation, we disrupted the actin cytoskeleton in human embryonic kidney (HEK) 293T cells using cytochalasin D, which blocks the addition of actin monomers to filaments (*18*), or latrunculin A, which binds actin monomers and prevents polymerization (Fig. 4A) (*19*). Inhibiting filamentous actin formation with either cytochalasin D or latrunculin A significantly reduced thermotolerance in human cells without causing death at permissive temperatures (Fig. 4B and fig. S10). Similar to our *C. elegans* data, these findings reiterate the importance of the actin cytoskeleton during times of cellular stress.

Elevated levels of *hsf-1* have been shown to benefit multiple organisms, yet its oncogenic properties are a major therapeutic drawback (*20*, *21*). Because the inducible chaperone network promotes survival and proliferation of metastasizing cells (*22*), the ability to harness protective, non-chaperone components within the HSF-1 signal transduction cascade appears essential for future drug development. Identification of *pat-10* as a modifier of thermotolerance and longevity may apply to mammalian systems without the typical oncogenic dangers associated with increased chaperone levels.

The *hsf-1(CT)* strain was still able to mount a transcriptional response to heat shock, albeit reduced in complexity of *hsf-1(FL)*. The molecular mechanism remains unclear by which *hsf-1(CT)* regulates transcription without the C-terminal activation domain, but possible explanations include HSF-1 containing multiple activation domains. Alternatively, the *hsf-1(CT)* modification may alter affinities to DNA-binding sites or different cofactors, which would modify the transcriptional profile.

Our findings underscore the importance of maintaining filamentous actin, as opposed to total levels of actin. We propose a model in which HSF-1 regulates chaperones and actin cytoskeletal genes in parallel to promote thermotolerance and longevity (Fig. 4C). In the absence of chaperone induction, stabilization of the actin cytoskeleton is sufficient to promote survival under conditions of cellular stress and aging.

REFERENCES AND NOTES

1. A.-L. Hsu, C. T. Murphy, C. Kenyon, *Science* **300**, 1142–1145 (2003).
2. M. Fujimoto *et al.*, *J. Biol. Chem.* **280**, 34908–34916 (2005).
3. G. McColl *et al.*, *Cell Metab.* **12**, 260–272 (2010).
4. N. Kourtis, V. Nikoletopoulou, N. Tavernarakis, *Nature* **490**, 213–218 (2012).
5. V. Prahlad, T. Cornelius, R. I. Morimoto, *Science* **320**, 811–814 (2008).
6. Y. M. Hajdu-Cronin, W. J. Chen, P. W. Sternberg, *Genetics* **168**, 1937–1949 (2004).
7. P. E. Kroeger, R. I. Morimoto, *Mol. Cell. Biol.* **14**, 7592–7603 (1994).
8. N. D. Trinklein, J. I. Murray, S. J. Hartman, D. Botstein, R. M. Myers, *Mol. Biol. Cell* **15**, 1254–1261 (2004).
9. H. Terami *et al.*, *J. Cell Biol.* **146**, 193–202 (1999).
10. K. Ono, S. Ono, *Mol. Biol. Cell* **15**, 2782–2793 (2004).
11. T. Obinata, K. Ono, S. Ono, *J. Cell Sci.* **123**, 1557–1566 (2010).
12. Z. Balklava, S. Pant, H. Fares, B. D. Grant, *Nat. Cell Biol.* **9**, 1066–1073 (2007).
13. T. Kuwahara *et al.*, *Hum. Mol. Genet.* **17**, 2997–3009 (2008).
14. L. A. Herndon *et al.*, *Nature* **419**, 808–814 (2002).
15. W. Greene, S.-J. Gao, *PLOS Pathog.* **5**, e1000512 (2009).
16. H. Fares, I. Greenwald, *Nat. Genet.* **28**, 64–68 (2001).
17. A. Patton *et al.*, *Curr. Biol.* **15**, 1045–1050 (2005).
18. J. F. Casella, M. D. Flanagan, S. Lin, *Nature* **293**, 302–305 (1981).
19. I. Spector, N. R. Shochet, Y. Kashman, A. Groweiss, *Science* **219**, 493–495 (1983).
20. L. Whitesell, S. Lindquist, *Expert Opin. Ther. Targets* **13**, 469–478 (2009).
21. C. H. Nguyen *et al.*, *Biochem. J.* **452**, 321–329 (2013).
22. D. R. Ciocca, A. P. Arrigo, S. K. Calderwood, *Arch. Toxicol.* **87**, 19–48 (2013).

ACKNOWLEDGMENTS

Bioinformatic analysis is included in the supplementary materials. The following funding sources supported this research: Howard Hughes Medical Institute, National Center for Research Resources (5P41RR011823-17), National Institute of General Medical Sciences (8 P41 GM103533-17), and National Institute on Aging (R01AG027463-04). N.A.B. was funded by a postdoctoral fellowship to the Salk Center for Nutritional Genomics from the Leona M. & Harry B. Helmsley Charitable Trust; P.M.D. was funded by George E. Hewitt Foundation for Medical Research and National Institute of Aging (1K99AG042495-01A1). We thank the laboratory of G. Lithgow for generously sharing the HSP-16 antibody and J. Durieux for helping design figure illustrations. Some of the nematode strains used in this work were provided by the *Caenorhabditis* Genetics Center (University of Minnesota), which is supported by the NIH–Office of Research Infrastructure Programs (P40 OD010440).

SUPPLEMENTARY MATERIALS

www.sciencemag.org/content/346/6207/360/suppl/DC1
Materials and Methods
Figs. S1 to S10
Tables S1
References (*23*–*40*)

10 March 2014; accepted 13 August 2014
10.1126/science.1253168

AUTOIMMUNITY

Detection of T cell responses to a ubiquitous cellular protein in autoimmune disease

Yoshinaga Ito,[1] Motomu Hashimoto,[1,2,3,4]* Keiji Hirota,[2]* Naganari Ohkura,[2,5] Hiromasa Morikawa,[2] Hiroyoshi Nishikawa,[2] Atsushi Tanaka,[2,5] Moritoshi Furu,[3,6] Hiromu Ito,[3,6] Takao Fujii,[3,4] Takashi Nomura,[1] Sayuri Yamazaki,[7] Akimichi Morita,[7] Dario A. A. Vignali,[8,9] John W. Kappler,[10,11] Shuichi Matsuda,[6] Tsuneyo Mimori,[4] Noriko Sakaguchi,[2] Shimon Sakaguchi[1,2,12]†

T cells that mediate autoimmune diseases such as rheumatoid arthritis (RA) are difficult to characterize because they are likely to be deleted or inactivated in the thymus if the self antigens they recognize are ubiquitously expressed. One way to obtain and analyze these autoimmune T cells is to alter T cell receptor (TCR) signaling in developing T cells to change their sensitivity to thymic negative selection, thereby allowing their thymic production. From mice thus engineered to generate T cells mediating autoimmune arthritis, we isolated arthritogenic TCRs and characterized the self antigens they recognized. One of them was the ubiquitously expressed 60S ribosomal protein L23a (RPL23A), with which T cells and autoantibodies from RA patients reacted. This strategy may improve our understanding of the underlying drivers of autoimmunity.

T cells mediate a variety of autoimmune diseases (*1*, *2*), likely through the recognition of self antigens. However, identification of the self antigens targeted by T cells in systemic autoimmune diseases such as rheumatoid arthritis (RA) has been technically difficult (*3*–*5*). This is because pathogenic T cells expressing high-affinity T cell receptors (TCRs) for ubiquitous self antigens may be largely deleted (i.e., negatively selected) in the thymus and

[1]Department of Experimental Pathology, Institute for Frontier Medical Sciences, Kyoto University, Kyoto 606-8507, Japan. [2]Department of Experimental Immunology, Immunology Frontier Research Center, Osaka University, Suita 565-0871, Japan. [3]Department of the Control for Rheumatic Diseases, Graduate School of Medicine, Kyoto University, Kyoto 606-8507, Japan. [4]Department of Rheumatology and Clinical Immunology, Graduate School of Medicine, Kyoto University, Kyoto 606-8507, Japan. [5]Department of Frontier Research in Tumor Immunology, Center of Medical Innovation and Translational Research, Osaka University, Osaka 565-0871, Japan. [6]Department of Orthopaedic Surgery, Graduate School of Medicine, Kyoto University, Kyoto 606-8507, Japan. [7]Department of Geriatric and Environmental Dermatology, Graduate School of Medical Sciences, Nagoya City University, Nagoya 467-8601, Japan. [8]Department of Immunology, St. Jude Children's Research Hospital, Memphis, TN 38105, USA. [9]Department of Immunology, University of Pittsburgh School of Medicine, Pittsburgh, PA 15261, USA. [10]Integrated Department of Immunology, National Jewish Health, Denver, CO 80206, USA. [11]Howard Hughes Medical Institute, National Jewish Health, Denver, CO 80206, USA. [12]Core Research for Evolutional Science and Technology (CREST), Japan Science and Technology Agency, Tokyo 102-0075, Japan. *These authors contributed equally to this work. †Corresponding author. E-mail: shimon@ifrec.osaka-u.ac.jp

scarcely detectable in the periphery or, if detected, in an inactivated state (*6*). This can be circumvented by altering TCR signaling, which changes the sensitivity of developing T cells to thymic selection and results in new dominant self-reactive TCR specificities that are causative of systemic autoimmune diseases (*7*–*11*). For example, a hypomorphic point mutation of ζ-associated protein 70 (ZAP-70), a TCR-proximal signaling molecule, causes T cell–mediated spontaneous autoimmune arthritis in mice, which resembles RA (*8*).

To identify ubiquitously expressed self antigens commonly targeted in mouse and human systemic autoimmune disease, we first examined whether the arthritogenic $CD4^+$ T helper (T_H) cells in BALB/c SKG mice, which develop autoimmune arthritis due to the ZAP-70 mutation, made use of a specific dominant TCR. We compared the arthritogenic capacity of SKG $CD4^+$ T cells expressing different TCR Vβ subfamilies (fig. S1). Transfer of SKG $CD4^+$ T cells expressing Vβ6, Vβ8.1/8.2, or Vβ10 into BALB/c *Rag2*$^{-/-}$ mice induced arthritis with similar severities. In addition, CDR3 gene segments of $V\beta6^+$ $CD4^+$ T cells in arthritic joints were diverse, with few common sequences among individual arthritic SKG mice (fig. S2 and tables S1 and S2). Thus, under the assumption that arthritogenic SKG $CD4^+$ T cells are highly polyclonal and make use of various Vα and Vβ TCR chains, we attempted to isolate a single arthritogenic $CD4^+$ T cell from a particular $CD4^+$ T cell subpopulation—for example, those expressing Vα2 and Vβ6, which constituted ~1% of joint-infiltrating $CD4^+$ T cells. To differentiate arthritogenic $CD4^+$ T cells from forkhead box P3 (Foxp3)–expressing $CD4^+$ regulatory T (T_{reg}) cells (*1*), we used SKG mice with knock-in of enhanced green fluorescent protein (EGFP)–Foxp3 fusion protein, designated eFOX SKG mice, which also spontaneously developed arthritis (fig. S3). We cloned a single TCR pair

A

Clone	Vα	Jα	CDR3	Vβ	Jβ	CDR3	Arthritogenic	Positive cells / Analyzed cells
1-23	14D-3/DV8*03	26*01	CAAS KG YAQGLTF	19*01	2-4*01	CASSI GGTGP SQNTLYF	No	1 / 12 (8.3%)
7-39	14D-3/DV8*03	40*01	CA AIY TGNYKYVF	19*01	2-1*01	CASS WRWGGER AEQFF	Yes	27 / 30 (90%)
6-39	14D-3/DV8*03	52*01	CAAS AA GANTGKLTF	19*01	2-7*01	CAS TPTF SYEQYF	Yes	2 / 26 (8%)

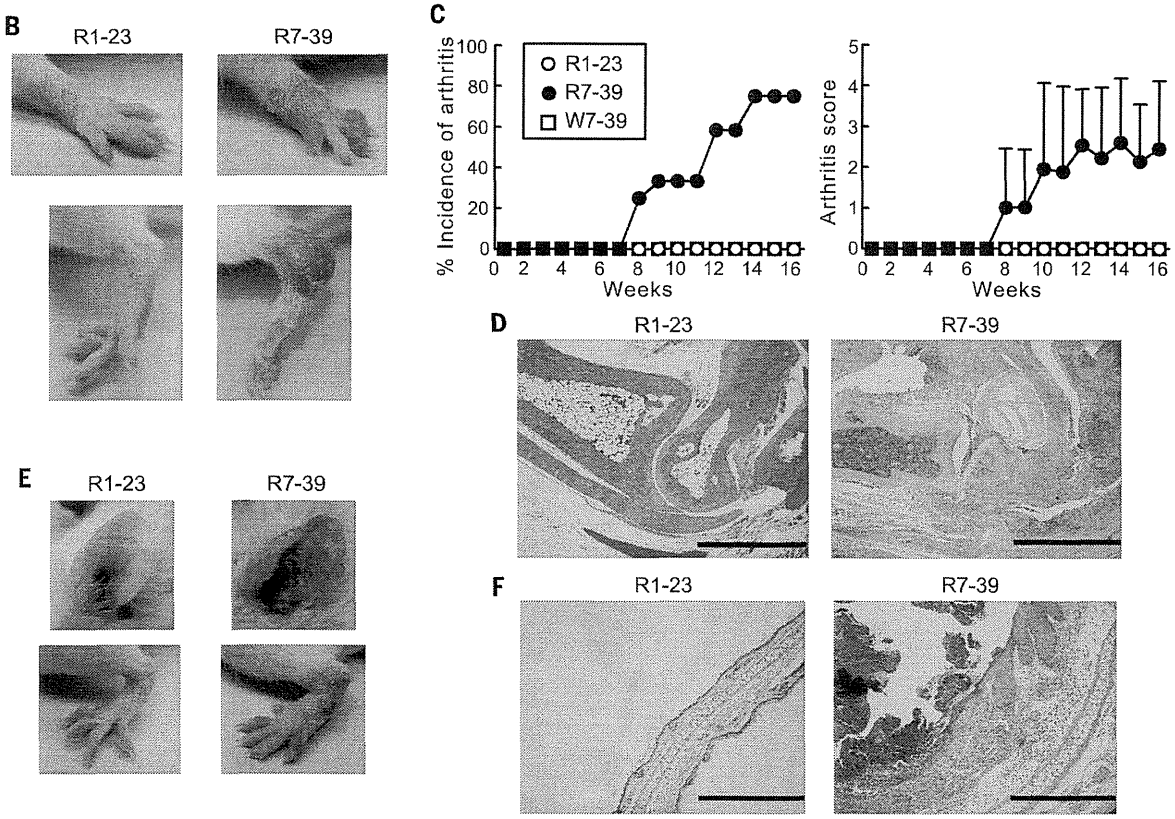

Fig. 1. Arthritis-inducing activity of two TCRs individually expressed in retrogenic mice. (**A**) Amino acid sequences and frequencies of two arthritogenic TCRs (7-39 and 6-39) and the nonarthritogenic 1-23 TCR. These three TCRs were obtained from three different mice. CDR, complementarity-determining region. Amino acid abbreviations: A, Ala; C, Cys; E, Glu; F, Phe; G, Gly; I, Ile; K, Lys; L, Leu; N, Asn; P, Pro; Q, Gln; R, Arg; S, Ser; T, Thr; V, Val; W, Trp; Y, Tyr. (**B**) Joint swelling in R7-39 retrogenic mice. (**C**) Incidence and scores of spontaneous arthritis in R7-39 (n = 11), R1-23 (n = 14), and W7-39 mice (n = 8). Error bars indicate means ± SD. (**D**) Hematoxylin and eosin (HE) staining of arthritic joints; scale bar, 1 mm. (**E**) Ears and hind paws of R7-39 and R1-23 mice. (**F**) HE staining of ears from R7-39 and R1-23 mice; scale bar, 500 μm. Results in (B) and in (D) to (F) represent three independent experiments.

from individual GFP$^-$ Vα2$^+$ Vβ6$^+$ CD4$^+$ T cells present in arthritic joints of eFOX SKG mice, transfected *Rag2*$^{-/-}$ SKG bone marrow (BM) cells with the TCR gene, and transferred the BM cells into *Rag2*$^{-/-}$ mice to construct retrogenic mice expressing the TCR pair in developing T cells (*12*–*15*). Among nine retrogenic strains each expressing a distinct TCR, those expressing 7-39 or 6-39 TCRs spontaneously developed arthritis at incidences of 80.0% and 27.3%, respectively (Fig. 1, A to C, and fig. S4, A to C). The two arthritogenic TCRs and a control nonarthritogenic 1-23 TCR used the same Vα and Vβ gene segments but different Jα and Jβ genes and CDR3 sequences (Fig. 1A). Arthritic joints in retrogenic 7-39 (R7-39) mice showed mononuclear cell infiltration, pannus formation, and cartilage destruction (Fig. 1D). Some (66.7%) of the R7-39, but not the R6-39, mice also developed chronic dermatitis, which exhibited hyperkeratosis and parakeratosis, histopathological features of human psoriasis (*16*) (Fig. 1, E and F, and fig. S5). Other organs were histologically intact (fig. S6).

In R7-39 mice, 7-39 TCR–transduced cells preferentially differentiated into monoclonal CD4$^+$ T cells with an activated and memory phenotype (fig. S7), and were able to transfer both arthritis and dermatitis into other *Rag2*$^{-/-}$ mice. Both arthritic R7-39 and nonarthritic R1-23 mice failed to develop Foxp3$^+$ T$_{reg}$ cells (fig. S8). In contrast to 7-39 TCR gene–transfected *Rag2*$^{-/-}$ BM cells with the SKG ZAP-70 mutation, 7-39 TCR gene–transfected ZAP-70–intact *Rag2*$^{-/-}$ BALB/c BM cells did not cause arthritis in retrogenic mice (designated W7-39 mice). In W7-39 mice, the majority of 7-39 TCR–expressing CD4$^+$ T cells were negatively selected in the thymus, and those that had escaped thymic negative selection exhibited a naïve nonactivated phenotype, indicating their dormant or anergic state (Fig. 1C and fig. S9).

Taken together, these results demonstrate that CD4$^+$ T cells with a specific TCR mediate autoimmune arthritis and also dermatitis, and that more than one TCR specificity is individually able to confer T cell arthritogenicity.

We next constructed T cell hybridomas expressing 7-39 or 6-39 TCRs and attempted to determine the self antigens recognized by these TCRs. The 7-39 hybridoma cells produced interleukin-2 (IL-2) when stimulated by cell extracts not only from SKG fibroblast-like synoviocytes (FLSs) but also from P3U1 cells, a BALB/c plasma cell–derived cell line (fig. S10). In contrast, syngeneic antigen-presenting cells (APCs) were sufficient to induce IL-2 production by 6-39 hybridoma cells, indicating that the 6-39 TCRs recognized a self antigen constitutively displayed by APCs (fig. S4D). To further characterize the self antigen recognized by 7-39 TCRs, we reconstituted *Rag2*$^{-/-}$ mice with a mixture of 7-39 TCR–transfected *Rag2*$^{-/-}$ SKG BM cells and *TCR*$\beta^{-/-}$ BALB/c BM cells on the assumption that the autoantibodies produced by B cells might specifically react with the self antigen recognized by 7-39 TCRs because T cell help came solely from 7-39 T$_H$ cells. The sera from these "B cell–reconstituted" mice specifically reacted with an 18-kD protein from the cell extract of P3U1 cells (Fig. 2A). Mass spectrometric analysis identified this protein as RPL23A, a component of the 60*S* subunit of ribosomes (*17*, *18*) (fig. S11). Various organs were found to express *RPL23A* mRNA at high levels (Fig. 2B). The amino acid sequence of RPL23A is 100% conserved between mice and humans (*18*). The sera from the B cell–reconstituted R7-39 mice indeed recognized recombinant RPL23A, but not histone H1.2 protein, another candidate protein indicated by the mass spectrometric analysis (Fig. 2C). In addition, recombinant RPL23A protein specifically stimulated the 7-39 hybridoma cells in a dose-dependent, class II major histocompatibility complex (MHC) I-A^d–dependent manner (Fig. 2D and fig. S12). Among 20-amino acid RPL23A peptides with consecutive overlapping of 5 amino acid residues, RPL23A$_{71\text{-}90}$ peptide stimulated 7-39 TCRs most potently (table S3 and fig. S13A).

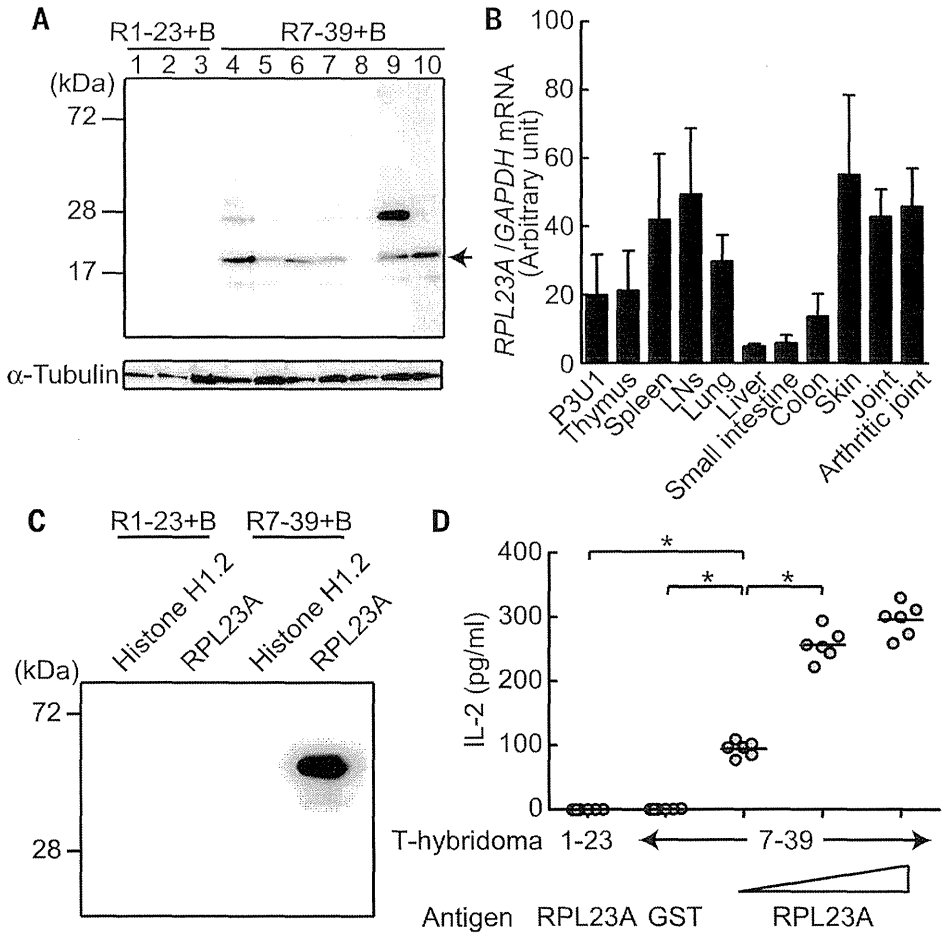

Fig. 2. Identification of the self antigen recognized by arthritogenic 7-39 TCRs. (**A**) Immunoblot analysis by sera from B cell–reconstituted R7-39 mice (n = 7) and B cell–reconstituted R1-23 mice (n = 3). Arrow indicates the commonly recognized protein. (**B**) Quantitative real-time polymerase chain reaction (qPCR) analysis for RPL23A gene expression in various tissues from SKG mice (n = 3). Error bars indicate means ± SD. (**C**) Recombinant RPL23A protein revealed by immunoblotting with sera from the indicated mice. (**D**) IL-2 production by 7-39 or 1-23 T cell hybridomas stimulated with the indicated recombinant proteins (n = 6). Horizontal bars indicate the means. *P < 0.05 (Kruskal-Wallis test followed by Steel-Dwass test). Results represent two [(A) to (C)] or three (D) independent experiments.

B cell–reconstituted R7-39 mice and arthritic SKG mice developed antibodies reacting with cyclic citrullinated peptides (CCP), as also observed in RA patients (*19*) (fig. S14A), yet there was no significant difference in titer of antibodies to RPL23A whether this was assessed with citrullinated or noncitrullinated RPL23A protein (fig. S14, B and C). In addition, the $RPL23A_{71\text{-}90}$ peptide recognized by 7-39 TCRs contained no arginine residue to be converted to citrulline (table S3).

Taken together, these results indicate that the ubiquitously expressed protein RPL23A can be a target antigen of both arthritis and dermatitis. Furthermore, more than one systemic antigen can be targeted for arthritis induction, because the 6-39 TCRs did not react to peptides derived from RPL23A (fig. S13B).

Upon transfer, $CD4^+$ T cells, but not sera, from B cell–reconstituted R7-39 mice induced arthritis in *Rag2*$^{-/-}$ mice (fig. S15). Indeed, $CD4^+$ T cells from arthritic joints or the regional lymph nodes of R7-39 mice produced inflammatory cytokines [including IL-17A, interferon-γ (IFN-γ), and granulocyte macrophage-colony stimulating factor (GM-CSF)] upon activation with phorbol 12-myristate 13-acetate (PMA) and ionomycin, RPL23A protein, or $RPL23A_{71\text{-}90}$ peptide (Fig. 3, A to D, fig. S16, A to D, and fig. S17). In addition, RPL23A stimulated nonarthritic SKG, but not BALB/c, $CD4^+$ T cells to produce IL-17A in vitro (Fig. 3E). It also augmented the production of IL-17A by $CD4^+$ T cells from SKG mice treated with mannan, which can trigger autoimmune arthritis in SKG mice by promoting T_H17 differentiation of arthritogenic $CD4^+$ T cells (*20*, *21*). An arthritic joint of SKG mice indeed harbored $CD4^+$ T cells possessing the Vβ CDR3 of 7-39 TCRs (table S2).

We next evaluated the contribution of T_{reg} cells to controlling arthritogenic $CD4^+$ T cells. T_{reg} cells

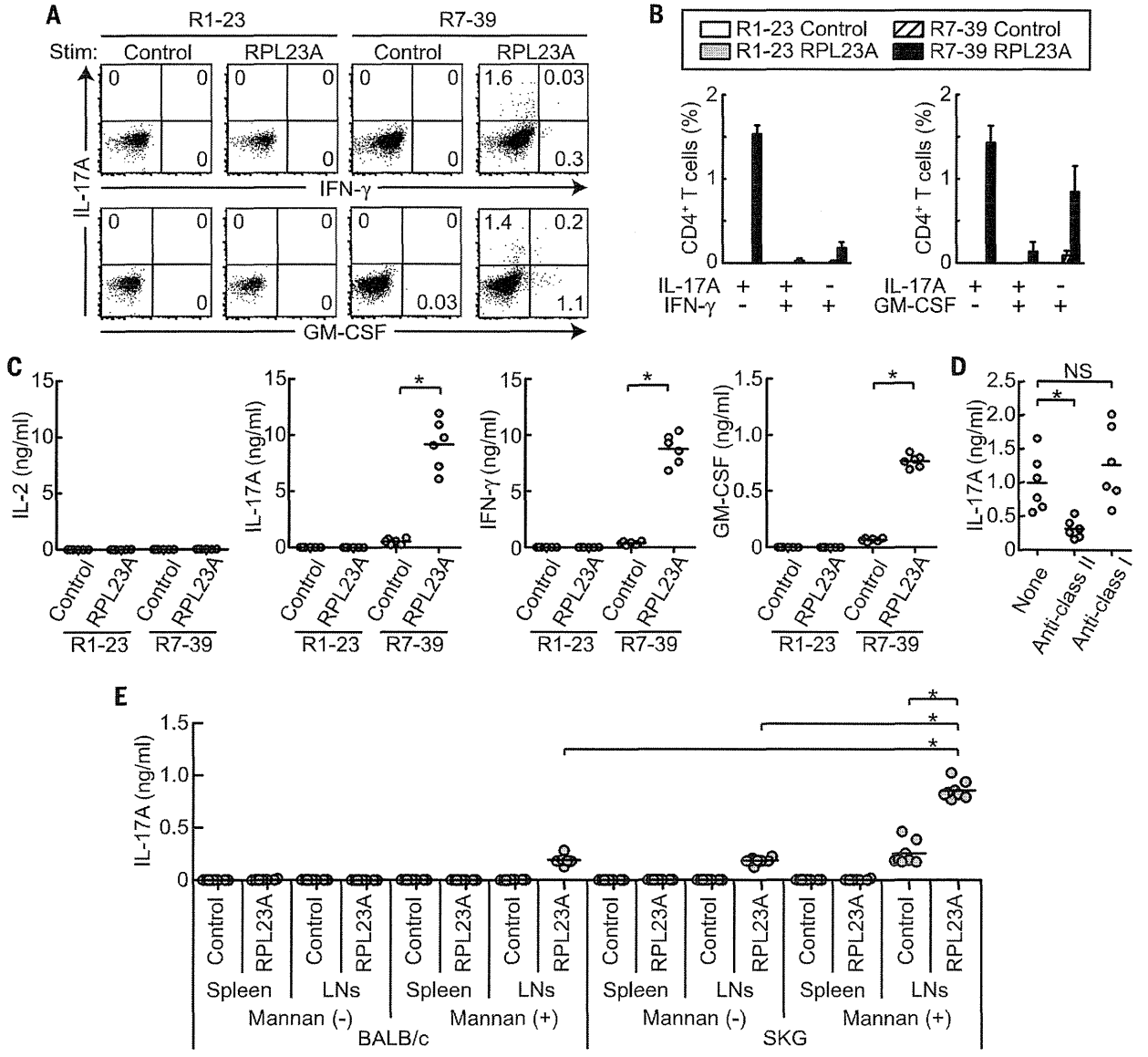

Fig. 3. RPL23A-reactive T_H cells in R7-39 mice. (**A**) Cytokine production by $CD4^+$ T cells from regional lymph nodes of R7-39 or R1-23 mice after in vitro stimulation with recombinant RPL23A or control glutathione *S*-transferase (GST) protein. Stim, stimulation. Data are representative of three independent experiments. (**B**) Percentages of cytokine-producing $CD4^+$ T cells in (A) ($n = 3$). (**C**) Cytokine amounts in culture supernatants in (A) ($n = 6$). (**D**) IL-17A production by RPL23A-stimulated lymphocytes from R7-39 mice in the presence or absence of blocking antibodies to MHC class I or class II ($n = 6$). (**E**) IL-17A production by lymphocytes stimulated with recombinant RPL23A or control GST proteins ($n = 8$). Lymphocytes were taken from SKG or BALB/c mice with or without mannan treatment. In (B), results are shown as means ± SD. In (C) to (E), horizontal bars indicate the means; $*P < 0.05$ (Kruskal-Wallis test followed by Steel-Dwass test); NS, not significant. Results represent two independent experiments in (B) and (C).

from either ZAP-70–intact BALB/c or ZAP-70–mutant SKG mice failed to suppress arthritis development in *Rag2*$^{-/-}$ mice when cotransferred with phenotypically activated or memory 7-39 TCR$^+$ CD4$^+$ T cells (figs. S7 and S18), although T_{reg} cells were capable of suppressing naïve arthritogenic T cells effectively (*9*).

These results collectively indicate that RPL23A is able to stimulate CD4$^+$ T cells in R7-39 mice via RPL23A-derived peptide–MHC class II complexes, driving them to differentiate into arthritogenic effector T_H cells (*20*), which are capable of mediating arthritis even in the presence of T_{reg} cells.

Lastly, we examined possible immune responses to RPL23A in RA patients. *RPL23A* mRNA was found to be ubiquitously expressed in healthy human tissues (Fig. 4A). In synovial tissues of RA patients and also in the apparently normal synovial tissues of osteoarthritis (OA) patients, RPL23A was detected in the cytoplasm of synovial cells, including CD55$^+$ FLSs (Fig. 4B). Relative to healthy controls (1.3%, n = 74), a significantly higher proportion of RA patients (16.8%, n = 374) were positive for serum immunoglobulin G–type autoantibodies to RPL23A (Fig. 4C). Two out of 23 psoriatic arthritis (PsA) patients (8.7%) were positive for the autoantibody, whereas all of the OA patients (n = 11), systemic lupus erythematosus (SLE) patients (n = 30), or

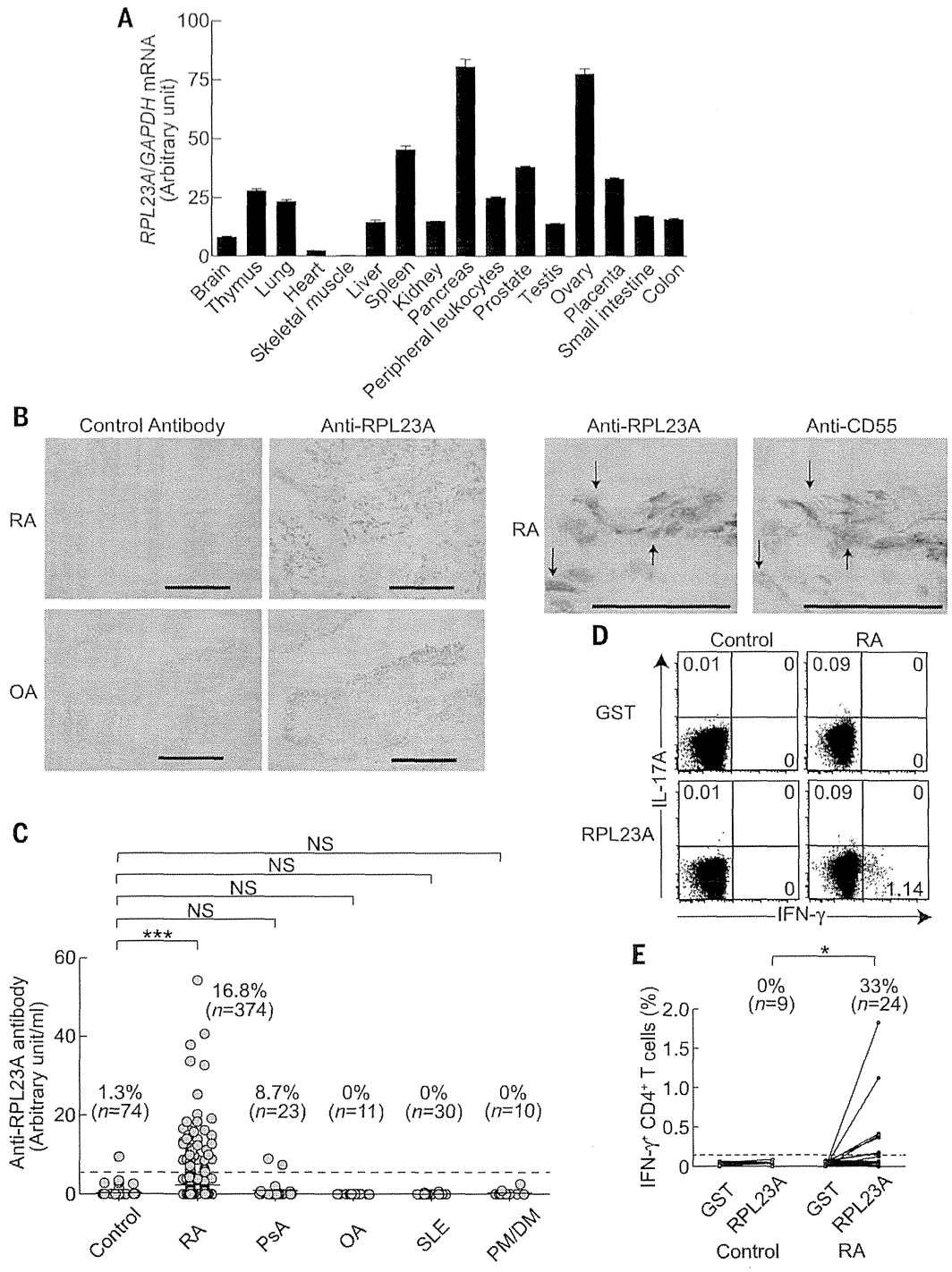

Fig. 4. Anti-RPL23A humoral and cellular immune responses in RA patients. (**A**) qPCR analysis of RPL23A gene expression in various tissues from healthy human subjects (n = 3). Results are shown as means ± SD and represent two independent experiments. (**B**) Immunohistochemical staining of synovial tissues from RA or OA patients for RPL23A or CD55 expression (scale bars, four images at left, 200 μm; two images at right, 50 μm). Serial sections were stained by anti-RPL23A, anti-CD55, or control antibody. Arrows indicate cells that are both RPL23A- and CD55-positive. Representative results from three patients are shown. (**C**) Serum levels of autoantibodies to RPL23A assessed by enzyme-linked immunosorbent assay (ELISA) in RA, PsA, OA, SLE, and PM/DM patients or healthy individuals. Horizontal bars indicate the medians. ***P < 0.001 (Kruskal-Wallis test followed by Dunn's multiple comparison test). (**D**) Cytokine production from CD4$^+$ T cells stimulated with recombinant RPL23A or GST protein. (**E**) Percentages of IFN-γ$^+$ cells in RPL23A- or GST-stimulated CD4$^+$ T cells in RA patients (n = 24) or healthy individuals (n = 9). *P < 0.05 (χ^2 test). Dashed lines indicate the threshold in (C) and (E).

polymyositis/dermatomyositis (PM/DM) patients (n = 10) were negative. In addition, in the synovial fluid of a subset of RA patients, we detected $CD4^+$ T cells producing IFN-γ upon stimulation with RPL23A (Fig. 4, D and E). These findings in humans, together with the key role of anti-RPL23A T cell responses for autoimmune arthritis and psoriasis-like dermatitis in mice, suggest that the responses may play a pathogenic role at least in a subset of patients with RA or PsA.

Our results show that by attenuating TCR signal intensity in developing T cells (hence reducing their sensitivity to thymic negative selection by natural self ligands), T cells reactive with ubiquitously expressed self antigens can be generated as dominant pathogenic clones causing systemic autoimmune disease. Because similar attenuation of TCR signaling at various degrees in conjunction with T_{reg} cell depletion is able to produce a variety of other autoimmune diseases in mice (*9*, *22*), this strategy of generating pathogenic T cells and characterizing the self antigens they recognize would facilitate our understanding of the mechanisms of other autoimmune diseases of currently unknown etiology. In addition, given that genetic polymorphism in a signaling molecule in T cells is a major determinant of genetic susceptibility to various human autoimmune diseases including RA (*23*), such a genetic variation might, at least in part, alter thymic selection, hence forming a TCR repertoire for causing autoimmune disease. Our approach may also be useful in deciphering how T cell autoimmunity to a ubiquitous self antigen triggers localized tissue damage in RA and other human autoimmune diseases, and in devising effective means of systemic or local intervention in the disease process.

REFERENCES AND NOTES

1. S. Sakaguchi, F. Powrie, R. M. Ransohoff, *Nat. Med.* **18**, 54–58 (2012).
2. P. Marrack, J. Kappler, B. L. Kotzin, *Nat. Med.* **7**, 899–905 (2001).
3. M. Feldmann, F. M. Brennan, R. N. Maini, *Cell* **85**, 307–310 (1996).
4. G. S. Firestein, *Nature* **423**, 356–361 (2003).
5. I. B. McInnes, G. Schett, *N. Engl. J. Med.* **365**, 2205–2219 (2011).
6. C. X. Chang *et al.*, *Front. Biosci.* **16**, 3014–3035 (2011).
7. L. Y. Hsu, Y. X. Tan, Z. Xiao, M. Malissen, A. Weiss, *J. Exp. Med.* **206**, 2527–2541 (2009).
8. N. Sakaguchi *et al.*, *Nature* **426**, 454–460 (2003).
9. S. Tanaka *et al.*, *J. Immunol.* **185**, 2295–2305 (2010).
10. C. L. Sommers *et al.*, *Science* **296**, 2040–2043 (2002).
11. O. M. Siggs *et al.*, *Immunity* **27**, 912–926 (2007).
12. J. Holst *et al.*, *Nat. Protoc.* **1**, 406–417 (2006).
13. G. P. Lennon *et al.*, *Immunity* **31**, 643–653 (2009).
14. M. L. Bettini, M. Bettini, M. Nakayama, C. S. Guy, D. A. Vignali, *Nat. Protoc.* **8**, 1837–1840 (2013).
15. See supplementary materials on *Science* Online.
16. F. O. Nestle, D. H. Kaplan, J. Barker, *N. Engl. J. Med.* **361**, 496–509 (2009).
17. K. Suzuki, I. G. Wool, *J. Biol. Chem.* **268**, 2755–2761 (1993).
18. W. Fan, M. Christensen, E. Eichler, X. Zhang, G. Lennon, *Genomics* **46**, 234–239 (1997).
19. W. J. van Venrooij, J. J. van Beers, G. J. Pruijn, *Nat. Rev. Rheumatol.* **7**, 391–398 (2011).
20. K. Hirota *et al.*, *J. Exp. Med.* **204**, 41–47 (2007).
21. M. Hashimoto *et al.*, *J. Exp. Med.* **207**, 1135–1143 (2010).
22. M. Ono, J. Shimizu, Y. Miyachi, S. Sakaguchi, *J. Immunol.* **176**, 4748–4756 (2006).
23. N. Bottini, T. Vang, F. Cucca, T. Mustelin, *Semin. Immunol.* **18**, 207–213 (2006).

ACKNOWLEDGMENTS

We thank D. O. Adeegbe, Y. Kitagawa, and K. Chen for critical reading of the manuscript; E. Yamamoto, M. Matsuura, R. Ishii, Y. Tada, Y. Funabiki, the technical support team (Graduate School of Medicine, Kyoto University), and K. Saito of DNA-chip Development Center for Infectious Diseases (RIMD, Osaka University) for technical assistance; T. Matsushita for histology; T. Kitamura for gifts of the packaging cell line Plat-E; the members of the Department of Rheumatology and Clinical Immunology, Kyoto University, for providing us with patients' sera; and the members of our laboratories for comments. The data presented in this paper are tabulated in the main paper and in the supplementary materials. eFOX mice and plasmids for making retrogenic mice are subject to a material transfer agreement. A patent application related to the work in this paper has been filed (PCT/JP2014/069306: A way to diagnose autoimmune arthritis; Y.I. and S.S. as inventors). Supported by Grants-in-Aid for Specially Promoted Research 20002007 (S.S. and Y.I.),;for Young Scientists (B) 24790996 (Y.I.) from the Japan Society for the Promotion of Science; Core Research for Evolutional Science and Technology from the Japan Science and Technology Agency (S.S.); NIH grant R01 DK089125 (D.A.A.V.); and American Lebanese Syrian Associated Charities (D.A.A.V.). M.H., T.F., M.F., H.I., and T.M. are affiliated with a department that is supported financially by five pharmaceutical companies (Mitsubishi Tanabe Pharma Co., Bristol-Myers K.K., Chugai Pharmaceutical Co. Ltd., AbbVie GK., and Eisai Co. Ltd.). The sponsors were not involved in the study design; in the collection, analysis, or interpretation of data; in the writing of this manuscript; or in the decision to submit the article for publication.

SUPPLEMENTARY MATERIALS

www.sciencemag.org/content/346/6207/363/suppl/DC1
Materials and Methods
Supplementary Text
Figs. S1 to S18
Tables S1 to S3
References (*24*–*36*)

22 July 2014; accepted 16 September 2014
10.1126/science.1259077

CellPress

Immunity
Article

Interleukin-10-Producing Plasmablasts Exert Regulatory Function in Autoimmune Inflammation

Masanori Matsumoto,[1,4] Akemi Baba,[1] Takafumi Yokota,[5] Hiroyoshi Nishikawa,[2] Yasuyuki Ohkawa,[7] Hisako Kayama,[3,6] Axel Kallies,[8,9] Stephen L. Nutt,[8,9] Shimon Sakaguchi,[2] Kiyoshi Takeda,[3,6] Tomohiro Kurosaki,[1,4,*] and Yoshihiro Baba[1,4,*]
[1]Laboratory for Lymphocyte Differentiation
[2]Laboratory for Experimental Immunology
[3]Laboratory for Immune Regulation
WPI Immunology Frontier Research Center, Osaka University, Suita, Osaka 565-0871, Japan
[4]Laboratory for Lymphocyte Differentiation, RIKEN Center for Integrative Medical Sciences (IMS), Yokohama, Kanagawa 230-0045, Japan
[5]Department of Hematology and Oncology
[6]Department of Microbiology and Immunology
Graduate School of Medicine, Osaka University, Suita, Osaka 565-0871, Japan
[7]Department of Advanced Medical Initiatives, JST-CREST, Faculty of Medicine, Kyushu University, Fukuoka 812-8582, Japan
[8]The Walter and Eliza Hall Institute of Medical Research, Parkville, VIC 3050, Australia
[9]Department of Medical Biology, The University of Melbourne, Parkville, VIC 3010, Australia
*Correspondence: kurosaki@ifrec.osaka-u.ac.jp (T.K.), babay@ifrec.osaka-u.ac.jp (Y.B.)
http://dx.doi.org/10.1016/j.immuni.2014.10.016

SUMMARY

B cells can suppress autoimmunity by secreting interleukin-10 (IL-10). Although subpopulations of splenic B lineage cells are reported to express IL-10 in vitro, the identity of IL-10-producing B cells with regulatory function in vivo remains unknown. By using IL-10 reporter mice, we found that plasmablasts in the draining lymph nodes (dLNs), but not splenic B lineage cells, predominantly expressed IL-10 during experimental autoimmune encephalomyelitis (EAE). These plasmablasts were generated only during EAE inflammation. Mice lacking plasmablasts by genetic ablation of the transcription factors Blimp1 or IRF4 in B lineage cells developed an exacerbated EAE. Furthermore, IRF4 positively regulated IL-10 production that can inhibit dendritic cell functions to generate pathogenic T cells. Our data demonstrate that plasmablasts in the dLNs serve as IL-10 producers to limit autoimmune inflammation and emphasize the importance of plasmablasts as IL-10-producing regulatory B cells.

INTRODUCTION

In the context of autoimmune disorders, B cells can be pathogenic effectors through their production of autoantibodies. However, evidence is accumulating that B cells can also be immunosuppressive in T-cell-mediated autoimmune and inflammatory diseases. Examples are collagen-induced arthritis (CIA) (Mauri et al., 2003), systemic lupus erythematosus (SLE) (Watanabe et al., 2010), and experimental autoimmune encephalomyelitis (EAE), an animal model of human multiple sclerosis (MS) (Fillatreau et al., 2002; Matsushita et al., 2008). The regulatory function of B cells is considered to be mainly determined by the secretion of interleukin-10 (IL-10), which is controlled by signals from Toll-like receptors (TLRs) (Lampropoulou et al., 2008), CD40 (Mauri et al., 2003), and B cell antigen receptors (BCR) (Fillatreau et al., 2002). To date, several unique populations of splenic IL-10-competent B cells (regulatory B cells) have been described. They include CD21^{hi}CD23^{hi}IgM^{hi} transitional 2-marginal zone precursor (T2-MZP) B cells (Evans et al., 2007) and CD1d^{hi}CD5^{+} B cells (Matsushita et al., 2008) that have been reported to inhibit autoimmunity. In addition, splenic CD138^{+} plasma cells were also reported to express IL-10 (Shen et al., 2014). However, these populations produce detectable IL-10 only when stimulated ex vivo. Thus, despite progress made in understanding the importance of B-cell-derived IL-10, there has been no definitive identification of in vivo IL-10-producing B cells with regulatory function during autoimmunity.

In humans, a role for B-cell-derived IL-10 in downregulation of inflammatory reactions has been suggested in autoimmune diseases such as MS or SLE (Blair et al., 2010; Duddy et al., 2007; Mauri and Bosma, 2012). Treatment with rituximab for B cell depletion efficiently ameliorated the disease progression in some autoimmune diseases, presumably because of elimination of pathogenic B cells (Gürcan et al., 2009). However, this might work in part because of selective survival and repopulation of regulatory B cell subsets (Duddy et al., 2007; Todd et al., 2014). The functional and clinical importance of human IL-10-competent B cells has begun to be elucidated but more must be learned about their characteristics.

Here we have exploited IL-10 reporter mice to identify in vivo IL-10-producing B cells and demonstrate that CD138^{+} plasmablasts, proliferating immature plasma cells, are the predominant source of IL-10 during EAE development. IL-10-producing plasmablasts were generated specifically in the draining lymph nodes (dLNs) but not in the spleen after EAE induction. By genetic

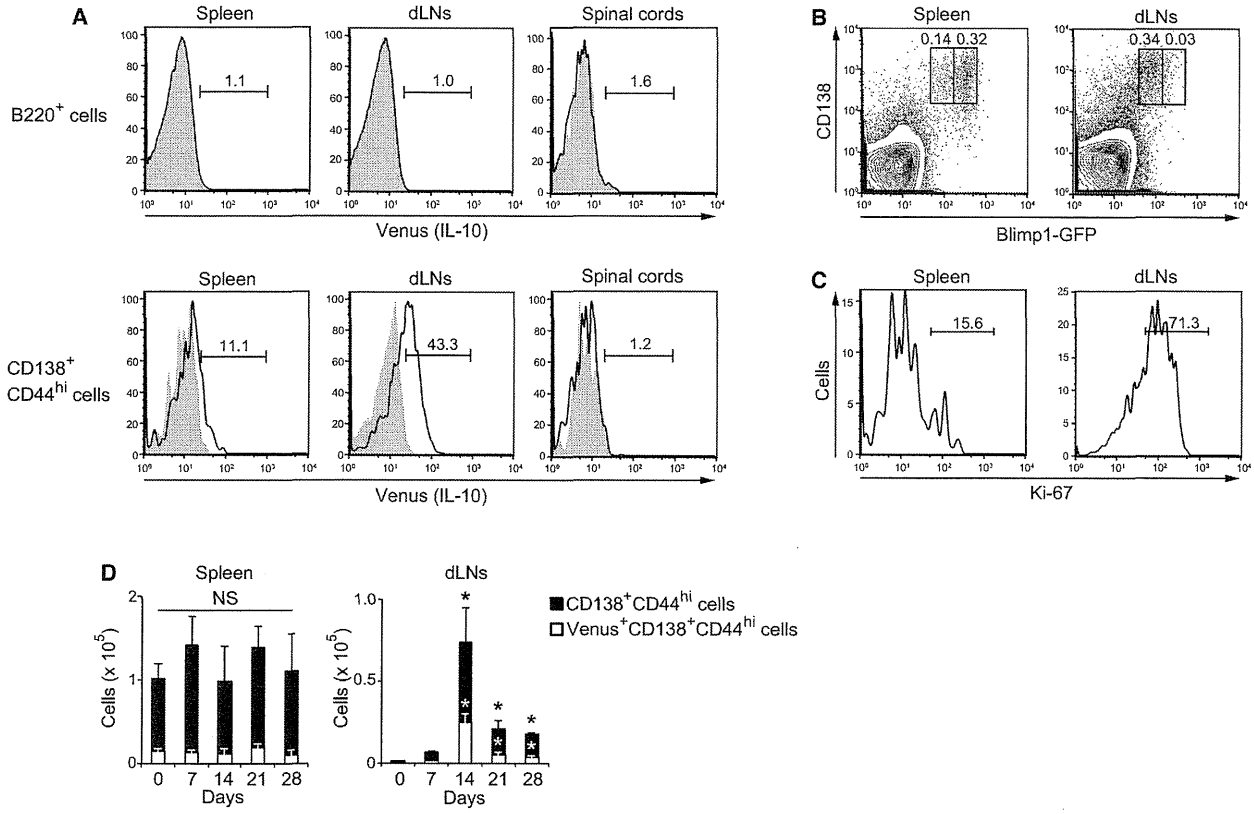

Figure 1. Plasmablasts Are the Dominant IL-10-Producing B Lineage Cells during EAE

(A) Flow cytometry of Venus expression in $B220^+$ and $CD138^+CD44^{hi}$ cells harvested from spleen, dLNs, and spinal cords of wild-type (shaded histogram) and $Il10^{Venus/+}$ (open histogram) mice 14 days after MOG_{35-55} immunization. Percentages of $Venus^+$ B cells are shown.

(B) Flow cytometry of cells from spleen and dLNs of $Prdm1^{gfp/+}$ mice 14 days after MOG_{35-55} immunization. GFP^{int} and GFP^{hi} populations of $CD138^+$ cells are gated and their percentages are shown.

(C) Flow cytometry of $CD138^+CD44^{hi}$ cells from spleen and dLNs of wild-type mice 14 days after MOG_{35-55} immunization. Percentages of Ki-67^+ cells are shown. Data are representative of at least three independent experiments in (A)–(C).

(D) Absolute number of $CD138^+CD44^{hi}$ or their $Venus^+$ cells from spleen and dLNs of $Il10^{Venus/+}$ mice before and 7, 14, 21, and 28 days after MOG_{35-55} immunization. Data are representative of two independent experiments. Data are presented as mean ± SEM for four mice. NS, not significant. *$p < 0.05$ versus day 0 (Welch's t test).

See also Figure S1.

approaches, we show that plasmablasts in the dLNs were critical for limiting EAE progression. In addition, IL-10 production by plasmablasts requires IRF4 and can prevent dendritic cells from generating pathogenic T cells. Furthermore, human plasmablasts also preferentially secrete IL-10, further highlighting plasmablasts as the IL-10-producing regulatory B cells.

RESULTS

Plasmablasts Are the Main IL-10-Producing B Cells during EAE

To identify in vivo IL-10-producing B cells and their distribution during autoimmune disease, we elicited EAE in mice carrying a transgene of *Venus*, a variant of yellow fluorescent protein ($Il10^{Venus/+}$), which allows tracking of $IL\text{-}10^+$ cells (Atarashi et al., 2011). Although previous reports suggested that several splenic B cell subsets can produce IL-10 (Mauri and Bosma, 2012; Yanaba et al., 2008), we observed little Venus expression in $B220^+$ B cells before and 14 days after immunization with myelin oligodendrocyte glycoprotein peptide (MOG_{35-55}) (Figure 1A and Figures S1A–S1D available online). In contrast, $CD138^+CD44^{hi}$ cells expressed Venus markedly in the dLNs, only modestly in spleen, and not at all in the spinal cords (Figures 1A, S1C, and S1D). ELISA assays also demonstrated that the $CD138^+CD44^{hi}$ population expressing Venus had a potential to produce IL-10 (Figure S1E). $CD138^+$ cells are composed of highly proliferative plasmablasts and nondividing plasma cells that express intermediate and high amounts of Blimp1 (encoded by the *Prdm1*), respectively (Kallies et al., 2004). By utilizing EAE-induced heterozygous $Prdm1^{gfp}$ knockin mice ($Prdm1^{gfp/+}$), we confirmed that $CD138^+$ cells in spleen and dLNs were largely GFP^{hi} plasma cells and GFP^{int} plasmablasts, respectively (Figure 1B). $CD138^+CD44^{hi}$ cells in dLNs, but not spleen, were proliferating, as demonstrated by Ki-67 staining

(Figure 1C). Whereas the absolute number of $CD138^+CD44^{hi}$ cells and their $Venus^+$ cells was essentially constant in spleen, those in dLNs expanded to a peak on day 14 after MOG_{35-55} immunization (Figure 1D). Thus, these results indicate that $CD138^+$ plasmablasts in dLNs are the principal IL-10-producing B lineage cells during EAE.

Plasmablasts in the dLNs Negatively Regulate EAE Inflammation

A key question is whether $IL\text{-}10^+CD138^+$ cells are functionally competent to inhibit EAE. To directly address this issue, we elicited EAE in mice conditionally lacking Blimp1 in B lineage cells by crossing of $Prdm1^{f/f}$ with $Mb1^{Cre/+}$ mice (called $Prdm1^{f/f}Mb1^{Cre/+}$ here). Plasma cell differentiation and antibody responses were impaired in these mice (Figures S2A and S2B). EAE development in $Prdm1^{f/f}Mb1^{Cre/+}$ mice was greatly exacerbated as compared to $Mb1^{Cre/+}$ control mice (Figure 2A). Consistent with the exacerbated EAE, $CD4^+$ T cells, particularly those producing interferon-γ (IFN-γ) (Th1 cells) and IL-17 (Th17 cells), increased in the spinal cords of $Prdm1^{f/f}Mb1^{Cre/+}$ mice (Figure 2B). When stimulated with MOG_{35-55}, $Prdm1^{f/f}Mb1^{Cre/+}$ LN cells produced more IFN-γ and IL-17 than $Mb1^{Cre/+}$ cells (Figure 2C). Thus, we conclude that $CD138^+$ plasmablasts/plasma cells limit EAE inflammation.

Given that IL-10-producing $CD138^+$ cells are detected in both spleen and dLNs during EAE, it remained important to test which secondary lymphoid organ is critical for EAE attenuation. L-selectin (CD62L), also known as Sell, is an essential homing receptor that governs migration into the peripheral LNs. To explore the involvement of LN B cells in EAE suppression, we generated mixed bone marrow (BM) chimeras by transferring a mixture of BM cells from μMT (80%) and $Sell^{-/-}$ (20%) mice into lethally irradiated wild-type mice. The Sell deficiency was restricted to B cells in the resultant BM chimera (B-$Sell^{-/-}$) mice. These mice lacked B lineage cells in LNs, but not spleen, and exhibited increased disease severity compared with control mice (Figure 2D). In striking contrast, mice that had splenectomy developed EAE normally (Figure 2E). B cell population and plasmablast differentiation in the dLNs was not affected by splenectomy. Collectively, these data suggest that plasmablasts in the dLNs negatively regulate EAE, but that splenic B lineage cells are dispensable for its suppression.

Nevertheless, published studies have claimed a functionally important role of splenic B cells to reduce EAE in adaptive transfer experiments (Fillatreau et al., 2002; Matsushita et al., 2008). Based on our above findings, we reasoned that adoptively transferred splenic B cells might give rise to plasmablasts in the dLNs that then regulate EAE. We therefore examined EAE in μMT mice with adoptively transferred splenic B cells isolated from $Prdm1^{f/f}Mb1^{Cre/+}$ or $Sell^{-/-}$ mice and control mice. Although the mice that received B cells from control mice resolved EAE symptoms, these suppressive effects were not observed when $Prdm1^{f/f}Mb1^{Cre/+}$ and $Sell^{-/-}$ B cells were transferred (Figures 2F and 2H). As expected, plasmablast differentiation from control B cells, but not $Prdm1^{f/f}Mb1^{Cre/+}$ and $Sell^{-/-}$ B cells, occurred in LNs (Figures 2G and 2I). These results suggest that splenic B cells can suppress EAE in an adoptive transfer setting but that their plasmablast differentiation in the dLNs might be required.

EAE Induces Generation of GC-Independent Plasmablasts that Produce IL-10 Preferentially

To gain insight into cellular aspects of IL-10-producing plasmablasts in the dLNs, we first investigated the cell surface phenotype. Most LN plasmablasts in EAE mice expressed high amounts of CD43, CXCR4, and major histocompatibility complex II (MHCII) and low amounts of B220, CD38, and CXCR5 (Figure 3A). Many of them also had undergone immunoglobulin (Ig) class-switch recombination (Figure 3B), which commonly occurs in both extrafollicular and germinal center (GC) responses (Klein and Dalla-Favera, 2008). Because an extensive expansion of GC B cells in the dLNs was detected during EAE (Figure 3C), we investigated the involvement of GCs in regulatory plasmablast generation. We elicited EAE in mice in which the transcription factor Bcl6 was functionally disrupted by inserting a YFP gene in both of the *Bcl6* alleles ($Bcl6^{yfp/yfp}$) (Kitano et al., 2011) and found that $Bcl6^{yfp/yfp}$ mice exhibited normal EAE despite of their lack of GC B cells (Figures 3D and 3E). The plasmablast generation was not significantly influenced by loss of Bcl6 (Figure 3E). Thus, EAE attenuation does not necessarily require GC responses.

We next assessed the potential contribution of anti-inflammatory cytokines besides IL-10 in plasmablasts. Because published studies have suggested that splenic B cells or plasma cells secrete IL-4, IL-13, IL-35, and transforming growth factor-β (TGF-β) (Mauri, 2010; Shen et al., 2014), we examined their expression in plasmablasts by quantitative RT-PCR analysis. In agreement with our data obtained with IL-10 reporter mice, $CD138^+CD44^{hi}$ plasmablasts, but not $CD19^+CD138^-$ B cells, highly expressed IL-10 (Figure 3F). By contrast, the amount of *Il4*, *Il13*, *Il27* (*Il27b/p28*), *Il35* (*Il12a/Il27b*), and *Tgfb1* mRNA in $CD138^+CD44^{hi}$ cells was decreased or comparable to that in $CD19^+$ cells. Consistent with that, ELISA and Bio-Plex suspension assay demonstrated preferential IL-10 secretion by $CD138^+CD44^{hi}$ cells (Figure 3G). Although IL-6 and IFN-γ produced by B cells have been reported to contribute to EAE pathogenesis (Barr et al., 2012; Matsushita et al., 2006), $CD138^+CD44^{hi}$ cells had little expression of their mRNA and proteins. Collectively, EAE-induced plasmablasts in the dLNs predominantly produce IL-10.

IRF4 Is Essential for Plasmablast IL-10 Production

We next investigated the mechanisms by which plasmablasts produce IL-10. In a previous study, we found that B cells could secrete IL-10 after BCR stimulation in a Ca^{2+} influx-dependent way (Matsumoto et al., 2011). However, this occurred only when B cells were preactivated with TLR agonists. Thus, we reasoned that TLR-dependent transcription factors would be required for plasmablast differentiation and/or IL-10 production. To this end, LPS-stimulated B cells from $Prdm1^{gfp/+}$ mice were sorted on the basis of GFP and CD138 expression followed by stimulation with anti-IgM (Figure 4A). IL-10 secretion was restricted to GFP^+ fractions and drastically enhanced by BCR ligation (Figure 4B). Because both $CD138^+GFP^+$ and $CD138^-GFP^+$ populations are known to have characteristics of antibody secretion and proliferative responses (Kallies et al., 2004), we concluded that plasmablasts are the principal IL-10 producers in vitro. Unexpectedly, however, B cells lacking Blimp1 proteins secreted IL-10 normally despite having impaired $CD138^+$

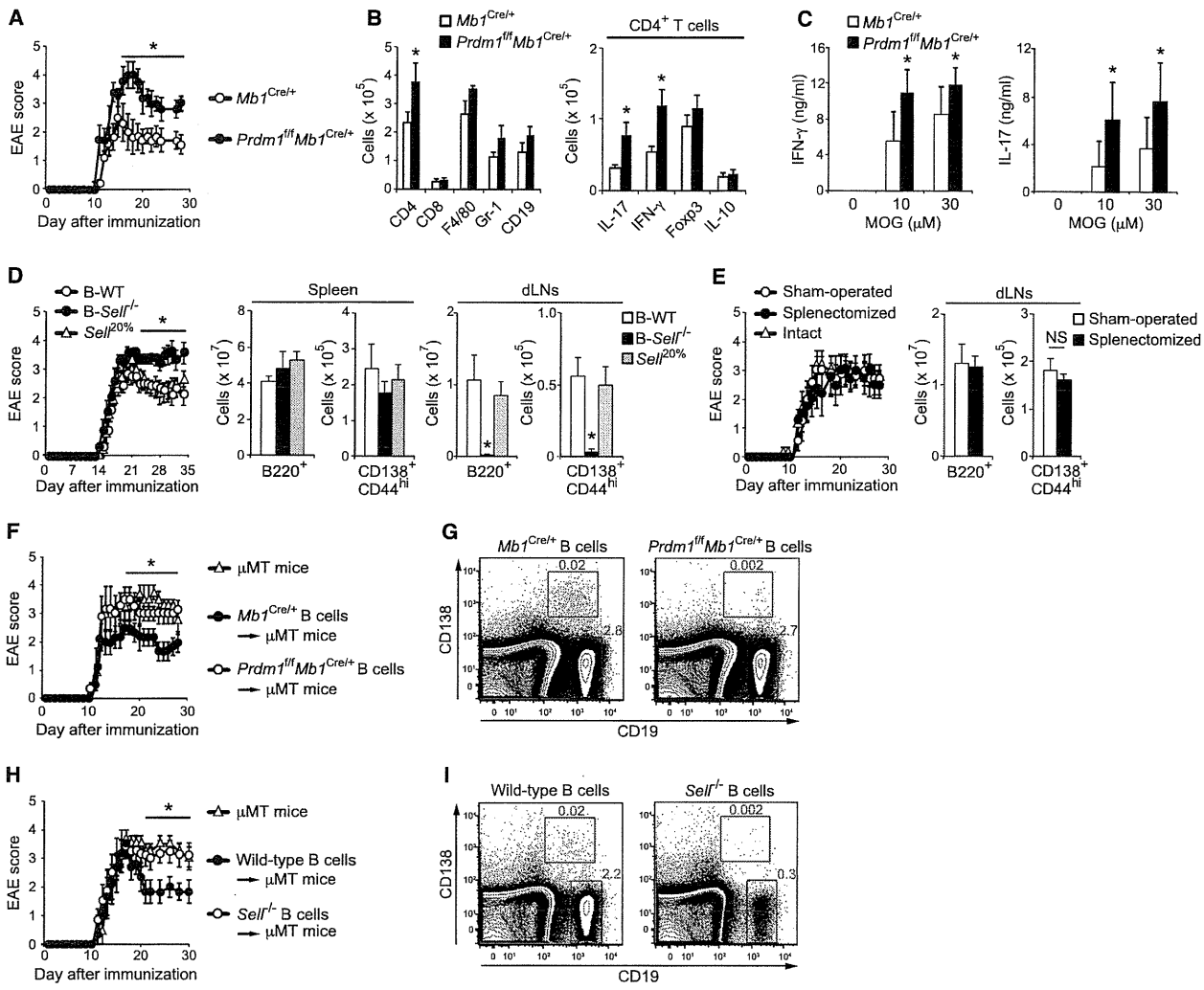

Figure 2. Plasmablasts in the dLNs Negatively Regulate EAE Inflammation

(A) Clinical EAE scores for $Mb1^{Cre/+}$ and $Prdm1^{f/f}Mb1^{Cre/+}$ mice immunized with MOG_{35-55}. The EAE score is shown as mean ± SEM for six to seven mice.

(B) Absolute number of cells from spinal cords harvested from $Mb1^{Cre/+}$ and $Prdm1^{f/f}Mb1^{Cre/+}$ mice 14 days after MOG_{35-55} immunization. Data are presented as mean ± SEM for five mice.

(C) ELISA of IFN-γ and IL-17 by cells isolated from the dLNs of $Mb1^{Cre/+}$ and $Prdm1^{f/f}Mb1^{Cre/+}$ mice 14 days after EAE induction followed by stimulation with MOG_{35-55} for 48 hr. Data are presented as mean ± SD.

(A–C) *p < 0.05 versus $Mb1^{Cre/+}$ mice (Mann-Whitney U test).

(D) Clinical EAE scores for B-$Sell^{-/-}$ (chimeric mice generated by transplanting a mixture of BM cells from μMT (80%) and $Sell^{-/-}$ (20%) mice and two control chimera groups: wild-type mice lethally irradiated and reconstituted with 80% μMT plus 20% wild-type bone marrow (B-WT) or reconstituted with 80% wild-type plus 20% $Sell^{-/-}$ bone marrow ($Sell^{20\%}$). The absolute number of $B220^+$ and $CD138^+CD44^{hi}$ cells harvested from spleen and dLNs of chimeras 14 days after MOG_{35-55} immunization is shown on the right. Data are shown as mean ± SEM for five to ten mice. *p < 0.05 versus B-WT mice (Mann-Whitney U test).

(E) Clinical EAE scores for sham-operated, splenectomized, and intact wild-type mice immunized with MOG_{35-55}. Absolute number of $B220^+$ and $CD138^+CD44^{hi}$ cells from dLNs of sham-operated and splenectomized mice 14 days after MOG_{35-55} immunization is shown on the right. Data are shown as mean ± SEM for five to seven mice. NS, not significant (Mann-Whitney U test).

(F) Clinical EAE scores for μMT mice immunized with MOG_{35-55} after injecting splenic B cells harvested from $Mb1^{Cre/+}$ and $Prdm1^{f/f}Mb1^{Cre/+}$ mice 28 days after EAE induction. The EAE score is shown as mean ± SEM for five to six mice. *p < 0.05 versus $Prdm1^{f/f}Mb1^{Cre/+}$ B cells (Mann-Whitney U test).

(G) Flow cytometry of cells from dLNs of μMT mice immunized for 12 days with MOG_{35-55} after injecting splenic $Mb1^{Cre/+}$ and $Prdm1^{f/f}Mb1^{Cre/+}$ B cells.

(H) Clinical EAE scores for μMT mice immunized with MOG_{35-55} after injecting splenic B cells harvested from wild-type and $Sell^{-/-}$ mice. The EAE score is shown as mean ± SEM for five to nine mice. *p < 0.05 versus $Sell^{-/-}$ B cells (Mann-Whitney U test).

(I) Flow cytometry of cells from dLNs of μMT mice immunized for 12 days with MOG_{35-55} after injecting splenic wild-type and $Sell^{-/-}$ B cells. $CD19^+$ and $CD138^+$ cells are gated and their percentages are shown (G and I).

Data are representative from three (A–D and F) or two (E and G–I) independent experiments. See also Figure S2.

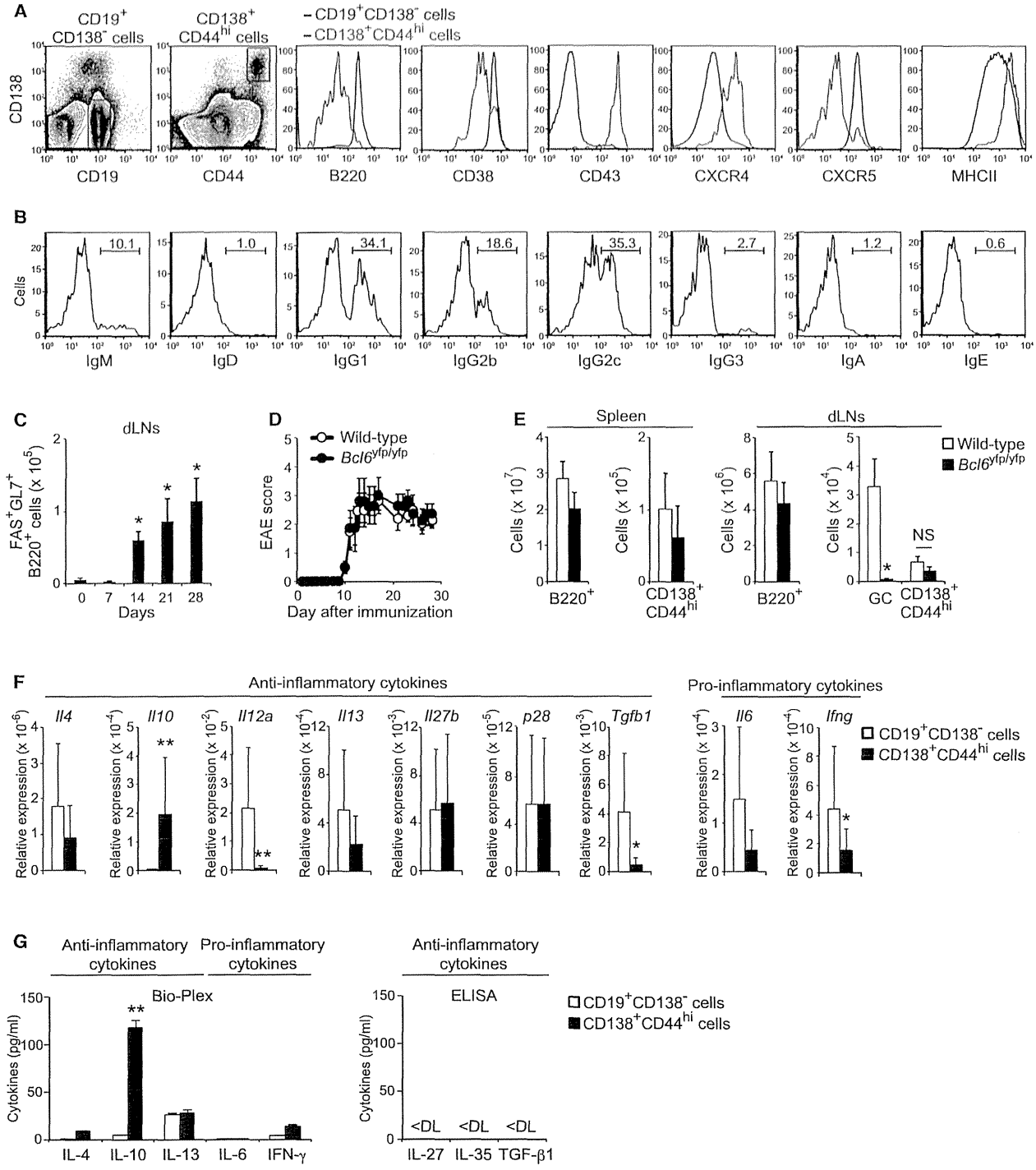

Figure 3. EAE Induces Generation of GC-Independent Plasmablasts that Produce IL-10 Preferentially

(A) Flow cytometry of $CD19^+CD138^-$ (black histogram, gated as in the left-most panel) and $CD138^+CD44^{hi}$ cells (red histogram, gated as in second panel from the left) harvested from dLNs of wild-type mice 14 days after MOG_{35-55} immunization.

(B) Flow cytometry of $CD138^+CD44^{hi}$ cells harvested from dLNs of wild-type mice 14 days after MOG_{35-55} immunization. Percentages of Ig^+ cells are shown.

(C) Absolute number of $FAS^+GL7^+B220^+$ (GC) B cells from dLNs harvested from wild-type mice before and 7, 14, 21, and 28 days after MOG_{35-55} immunization. Data are presented as mean ± SEM for five to six mice. *$p < 0.05$ versus day 0 (Mann-Whitney U test).

(D) Clinical EAE scores for wild-type and $Bcl6^{yfp/yfp}$ mice immunized with MOG_{35-55}. The EAE score is shown as mean ± SEM for seven mice.

(legend continued on next page)

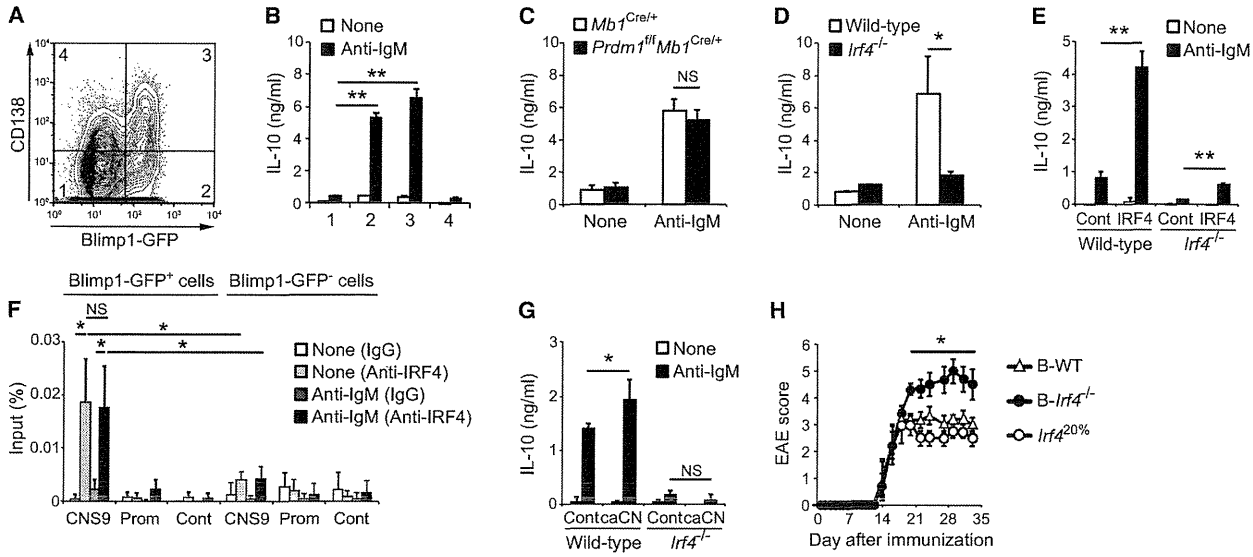

Figure 4. IRF4 Is Essential for Plasmablast IL-10 Production

(A) Flow cytometry of B cells isolated from spleen of *Prdm1*$^{gfp/+}$ mice and cultured with LPS for 48 hr. Four populations—GFP$^-$CD138$^-$ (fraction 1), GFP$^+$CD138$^-$ (fraction 2), GFP$^+$CD138$^+$ (fraction 3), and GFP$^-$CD138$^+$ (fraction 4) cells—were sorted and assayed in (B).

(B) ELISA of IL-10 secreted by the sorted B cells after stimulation with anti-IgM for 24 hr.

(C) ELISA of IL-10 secreted by B cells isolated from peripheral LNs of *Mb1*$^{Cre/+}$ and *Prdm1*$^{f/f}$*Mb1*$^{Cre/+}$ mice and cultured with LPS for 48 hr followed by stimulation with anti-IgM for 24 hr.

(D) ELISA of IL-10 secreted by B cells isolated from peripheral LNs of wild-type and *Irf4*$^{-/-}$ mice and cultured with LPS for 48 hr followed by stimulation with anti-IgM for 24 hr.

(E) ELISA of IL-10 secreted by GFP$^+$ cells sorted from LPS-activated wild-type and *Irf4*$^{-/-}$ B cells retrovirally transduced with GFP alone (Cont) or IRF4 followed by stimulation with anti-IgM for 24 hr.

(F) ChIP analysis of GFP$^+$ plasmablasts and GFP$^-$ B cells sorted from LPS-activated *Prdm1*$^{gfp/+}$ B cells, stimulated with anti-IgM for 30 min, and then precipitated with anti-IRF4 Ab or goat IgG. Input DNA and precipitated DNA were quantified by RT-PCR with PCR primers specific for CNS9 and promoter (Prom) regions of *Il10* or 3′ region of *Cd19* (Cont). Data shown are pooled from two independent experiments.

(G) ELISA of IL-10 secreted by GFP$^+$ cells sorted from LPS-activated wild-type and *Irf4*$^{-/-}$ B cells retrovirally transduced with GFP alone (Cont) or constitutively active calcineurin (caCN) followed by stimulation with anti-IgM for 24 hr. NS, not significant.

(H) Clinical EAE scores for chimeric mice in which only B cells lacked IRF4 (B-*Irf4*$^{-/-}$; wild-type mice lethally irradiated and reconstituted with 80% μMT plus 20% *Irf4*$^{-/-}$ bone marrow) and two control chimera groups: wild-type mice lethally irradiated and reconstituted with 80% μMT plus 20% wild-type bone marrow (B-WT) or reconstituted with 80% wild-type plus 20% *Irf4*$^{-/-}$ bone marrow (*Irf4*$^{20\%}$). The EAE score is shown as mean ± SEM for five to six mice. *$p < 0.05$ versus B-WT mice (Mann-Whitney U test).

(B–G) Data are presented as mean ± SD. *$p < 0.05$, **$p < 0.001$ (Student's t test).

Data are representative of three (A–E and G) or two (H) independent experiments. See also Figures S3 and S4.

cell generation (Figures 4C, S3A, and S3B), suggesting that Blimp1 in developing plasmablasts is dispensable for IL-10 production. Importantly, B cells lacking Blimp1 fail to fully differentiate into plasma cells, but rather initiate this differentiation pathway (Kallies et al., 2007; Kallies and Nutt, 2007; Shapiro-Shelef et al., 2003). Therefore, we next focused on the functional importance of IRF4 because it is a critical factor in the early phase of plasma cell differentiation and one of the downstream targets of TLR and BCR signaling (Mittrücker et al., 1997; Oracki et al., 2010). LPS-activated *Irf4*$^{-/-}$ B cells had impaired IL-10 secretion after BCR ligation (Figure 4D). Reciprocally, retroviral expression of IRF4 in wild-type B cells substantially increased IL-10 production and partially rescued it in *Irf4*$^{-/-}$ B cells (Figure 4E). Furthermore, chromatin immunoprecipitation (ChIP) analysis revealed that IRF4 in plasmablasts bound to the *Il10* CNS9 region, which controls *Il10* expression and is located approximately 9.1 kbp upstream of the transcription start site (Lee et al., 2009), though this binding frequency was unaffected by BCR stimulation (Figure 4F). These results imply that IRF4 not only induces plasmablast generation but also directly regulates *Il10* expression. Nuclear factor

(E) Absolute number of each B cell subset from spleen and dLNs harvested from wild-type and *Bcl6*$^{yfp/yfp}$ mice 28 days after MOG_{35-55} immunization. Data are presented as mean ± SEM for six mice. *$p < 0.05$ versus wild-type mice (Mann-Whitney U test). NS, not significant.

(F and G) Quantitative RT-PCR (F) and ELISA and Bio-Plex cytokine (G) analysis of CD19$^+$CD138$^-$ and CD138$^+$CD44^{hi} cells harvested from dLNs of wild-type mice 14 days after MOG_{35-55} immunization. For ELISA and Bio-Plex suspension assay, the isolated CD19$^+$CD138$^-$ and CD138$^+$CD44^{hi} cells were stimulated with PMA and ionomycin for 5 hr (G). Data are presented as mean ± SD. Abbreviations: <DL, below detection limit. *$p < 0.05$, **$p < 0.001$ versus CD19$^+$ cells (Student's t test).

Data are representative from three (A, B, and F) or two (C–E and G) independent experiments.

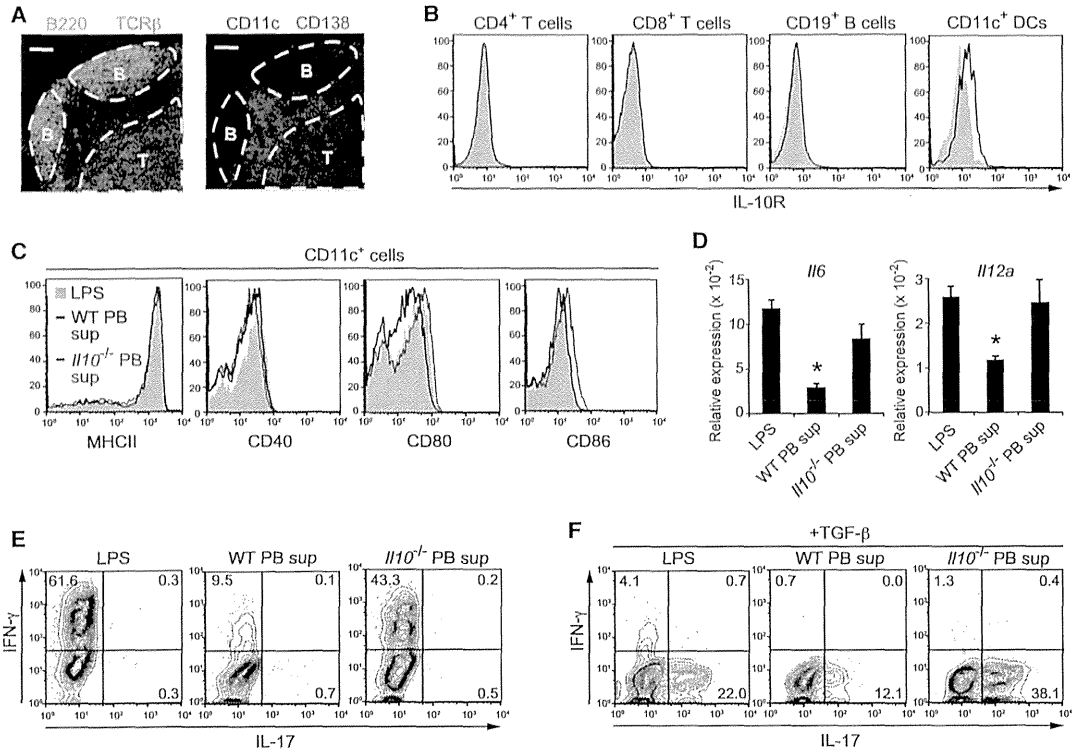

Figure 5. Plasmablasts Inhibit Dendritic Cell Function to Generate Autoreactive T Cells

(A) Histological analysis of dLNs harvested from wild-type mice 14 days after MOG_{35-55} immunization. Sections were stained with B220 and TCR-β Abs (left) or with CD11c and CD138 Abs (right). Original magnification, ×10; scale bars represent 100 μm.

(B) Flow cytometry of IL-10R expression by cells harvested from dLNs of wild-type mice 14 days after MOG_{35-55} immunization. Cells were stained with an IL-10R mAb (open histogram) or isotype control (shaded histogram).

(C) Flow cytometry of $CD11c^+$ cells harvested from dLNs of wild-type mice 14 days after MOG_{35-55} immunization followed by stimulation with LPS alone (shaded histogram) or supernatants from wild-type plasmablasts (PB) (WT PB sup; black histogram) and *Il10*$^{-/-}$ plasmablasts (*Il10*$^{-/-}$ PB sup; red histogram) activated with LPS and then anti-IgM.

(D) Quantitative RT-PCR analysis of *Il6* and *Il12a* transcripts in $CD11c^+$ cells harvested from dLNs of wild-type mice 14 days after MOG_{35-55} immunization, stimulated with LPS or WT and *Il10*$^{-/-}$ PB sup, normalized to the expression of *Gapdh*. Data are presented as mean ± SD. *$p < 0.05$ versus DC treated with *Il10*$^{-/-}$ PB sup (Student's t test).

(E and F) Cytokine profiles of TCR^{MOG}-expressing naive $CD4^+$ T cells cocultured with dLN $CD11c^+$ cells stimulated with LPS or WT and *Il10*$^{-/-}$ PB sup in the absence (E) or presence (F) of TGF-β together with MOG_{35-55} for 72 hr. Percentages of IFN-γ^+ and/or IL-17^+ cells are shown.

Results represent one of three similar experiments. See also Figure S5.

of activated T cells (NFAT), which is activated by Ca^{2+} and the calmodulin-dependent phosphatase calcineurin, is also vital for BCR-induced IL-10 production (Matsumoto et al., 2011). Retroviral expression of a constitutively active form of calcineurin A (caCN) markedly increased BCR-induced IL-10 production in an IRF4-dependent manner (Figure 4G), suggesting that NFAT-dependent IL-10 production requires IRF4. Moreover, we found that IRF4 has a B cell regulatory role in vivo because B-cell-specific *Irf4*-deficient chimeric mice lacking $CD138^+CD44^{hi}$ cells in the dLNs became susceptible to EAE (Figures 4H and S4). Together, these data indicate that IRF4 is essential for B cell IL-10 production to suppress EAE.

Plasmablast-Derived IL-10 Inhibits Dendritic Cell Function to Generate Pathogenic T Cells

We next elucidated the mechanisms by which plasmablasts suppress EAE. Immunohistochemical analysis of the dLNs in EAE-induced mice revealed that $CD138^+$ plasmablasts were mainly colocalized with $CD11c^+$ dendritic cells (DCs) in the extrafollicular region between T cell zones and B cell follicles (Figure 5A). Given that DCs, but not T and B cells, expressed detectable amounts of IL-10 receptor (IL-10R) (Figure 5B), we next examined whether DC function is affected by plasmablast-derived IL-10. When DCs were stimulated with supernatants derived from wild-type plasmablasts activated with LPS and then anti-IgM, the expression of MHCII, CD40, CD80, and CD86 was unchanged, but *Il6* and *Il12* mRNA was significantly decreased. This effect was not observed with *Il10*$^{-/-}$ plasmablasts (Figures 5C and 5D). Consistent with these results, Th1 cell differentiation of MOG-specific T cells was markedly prevented by supernatants from wild-type, but not *Il10*$^{-/-}$, plasmablasts when cocultured with DCs (Figure 5E). Very similar results were obtained with TGF-β-mediated Th17 cell generation (Figure 5F). Furthermore, we also observed equivalent results

when DCs were cocultured with Blimp1-GFP$^+$ plasmablasts (Figure S5). Thus, these results suggest that IL-10-producing plasmablasts inhibit DC functions to generate autoreactive T cells. This does not exclude the possibility that other cell types will be affected in vivo by plasmablast IL-10.

Human Plasmablasts Are IL-10-Producing B Cells

Our findings that plasmablasts represent the IL-10-producing B cells in mice led us to test whether this also applies to humans. B cells were isolated from peripheral blood of healthy donors and cultured with CpG (a TLR9 agonist) and/or cytokine cocktails including IL-2, IL-6, and interferon-alpha (IFN-α), which are known to provide conditions for effective plasmablast differentiation (Jego et al., 2003; Joo et al., 2012). Indeed, we detected CD27^{hi}CD38$^+$ putative plasmablasts after culture with CpG, while concomitant treatment with CpG and cytokine cocktails induced a greater frequency of an additional population of CD27^{int}CD38$^+$ cells as well as CD27^{hi}CD38$^+$ cells (Figure 6A). In particular, IFN-α was considerably effective for CD27^{int}CD38$^+$ differentiation and essentially the same results were obtained with IFN-β instead of IFN-α (Figure S6A). We found that IL-10 production was greatly induced in culture with a mixture of CpG and cytokine cocktails (Figure 6B). Both CD27^{hi}CD38$^+$ and CD27^{int}CD38$^+$ populations had a progressive loss of CD20, CD180, and Pax5 (Figures 6C, S6B, and S6C). Inversely, they had higher expression of IRF4, Blimp1, and XBP1 proteins and their transcripts (Figures 6C and S6C) and showed morphological maturation into plasma cells, as displayed by larger size with abundant cytoplasm, eccentric nuclei, and perinuclear haloes (Figure 6D). Consistent with these observations, both CD27^{hi}CD38$^+$ and CD27^{int}CD38$^+$ cells substantially secreted IgM (Figure 6E). Given the lack of a human mature plasma cell marker CD138 (Figure S6B), CD27^{int}CD38$^+$ cells as well as CD27^{hi}CD38$^+$ cells can be considered as plasmablasts whereas the CD27^{hi} cells apparently are more mature than CD27^{int} cells in view of their phenotypes. To determine which populations produce IL-10, we purified four fractions based on CD27 and CD38 expression after culture. ELISA assay showed that CD27^{int}CD38$^+$ plasmablasts selectively secreted IL-10 (Figure 6F). As a further test of this finding, we conducted IL-10 secretion assay by using IL-10 capture and detection antibodies, which allow us to detect live IL-10-secreting cells and found that the majority of IL-10$^+$ B cells consisted of CD27^{int}CD38$^+$ cell fraction (Figure 6G). Of note, this IL-10$^+$CD27^{int}CD38$^+$ population substantially secreted IgM, as assessed by ELISPOT assay (Figure 6H), suggesting that IL-10-producing B cells are Ig-secreting CD27^{int}CD38$^+$ plasmablasts.

We next addressed the issue of why CD27^{int}, but not CD27^{hi}, plasmablasts produce IL-10. Given that freshly prepared peripheral blood B cells consist of three major populations, i.e., CD24^{lo}CD27$^-$CD38$^-$ (naive mature), CD24^{hi}CD27$^-$CD38^{lo} (naive immature), and CD24^{hi}CD27$^+$CD38$^-$ (memory) cells (Figure 6I), the origin of each might be different. To test this hypothesis, they were sorted and then cultured. Memory B cells were predominantly differentiated into CD27^{hi}CD38$^+$ plasmablasts, whereas naive immature B cells and mature B cells, albeit to a lesser degree, became CD27^{int}CD38$^+$ plasmablasts (Figure 6I). Naive B-cell-derived CD27^{int} plasmablasts produced considerably more IL-10 (Figures 6J, S6D, and S6E). Collectively, these findings establish that human plasmablasts that arise from naive and especially immature B cells, but not memory B cells, are the major IL-10-producing B cells.

DISCUSSION

Our findings identify plasmablasts as the IL-10-producing B cells that can suppress autoimmunity. This was the case for EAE, where they were developed in the dLNs under the control of Blimp1 and IRF4 and disease progression was enhanced by their deletion. Furthermore, human plasmablasts also preferentially secreted IL-10, and these cells were derived from naive but not memory B cells.

It was previously thought that splenic B cells secrete the IL-10 that limits EAE. Instead, we found that CD138$^+$ plasmablasts in the dLNs were the major producers of this cytokine during EAE. This was the case when assessed by *Il10*$^{Venus/+}$ reporter mice or quantitative RT-PCR. In accordance with previous reports using several other IL-10 reporter lines injected with LPS or infected with *Salmonella* (Madan et al., 2009; Maseda et al., 2012; Shen et al., 2014), we also observed Venus expression in splenic CD138$^+$ cells in *Il10*$^{Venus/+}$ mice. However, amounts were very low and the frequency of positive cells was unaffected by EAE induction. By contrast, IL-10$^+$ plasmablasts in the dLNs were newly generated within extrafollicular foci, implying negative feedback regulation to protect excessive inflammation.

Our finding of severe EAE pathogenesis in the absence of plasmablasts due to B-cell-specific deletion of Blimp1 or IRF4 supports the idea that plasmablasts possess regulatory activity in vivo. This regulatory function is dependent on the dLNs and independent of the spleen. On the other hand, results from adoptive transfer studies were interpreted to mean that splenic B cells, especially the CD1d^{hi}CD5$^+$ B cell population, could suppress EAE through some unknown mechanism (Matsushita et al., 2008). Although we also observed that adoptive transfer of splenic B cells normalized EAE, plasmablast generation in the dLNs was required. CD1d^{hi}CD5$^+$ B cells extensively differentiate into plasmablasts in culture (Maseda et al., 2012) and their adoptive transfer from mice lacking IL-21R, CD40, and MHCII, which are indispensable for plasma cell differentiation (McHeyzer-Williams et al., 2012), into *Cd19*$^{-/-}$ mice does not resolve EAE development (Yoshizaki et al., 2012). Therefore, this population might serve as plasmablast precursors in an adoptive transfer setting.

The finding of in vitro BCR-dependent IL-10 production specifically in Blimp1$^+$ cells provides further evidence for the importance of plasmablasts and can explain the previously demonstrated need for TLR signaling for BCR-mediated IL-10 expression (Matsumoto et al., 2011). This idea is also supported by the observation of impaired IL-10 secretion in the absence of IRF4, which resulted in defective plasmablast differentiation (Figure S3A). Thus, IRF4 is required for IL-10 expression along with plasmablast differentiation in vitro and in vivo. Importantly, TLR and BCR signals induce the expression of IRF4 (De Silva et al., 2012) and therefore operate upstream of both plasmablast differentiation and IL-10 production. We detected deposition of IRF4 at the CNS9 region upstream enhancer in the *Il10* locus. This is in agreement with published studies that demonstrated

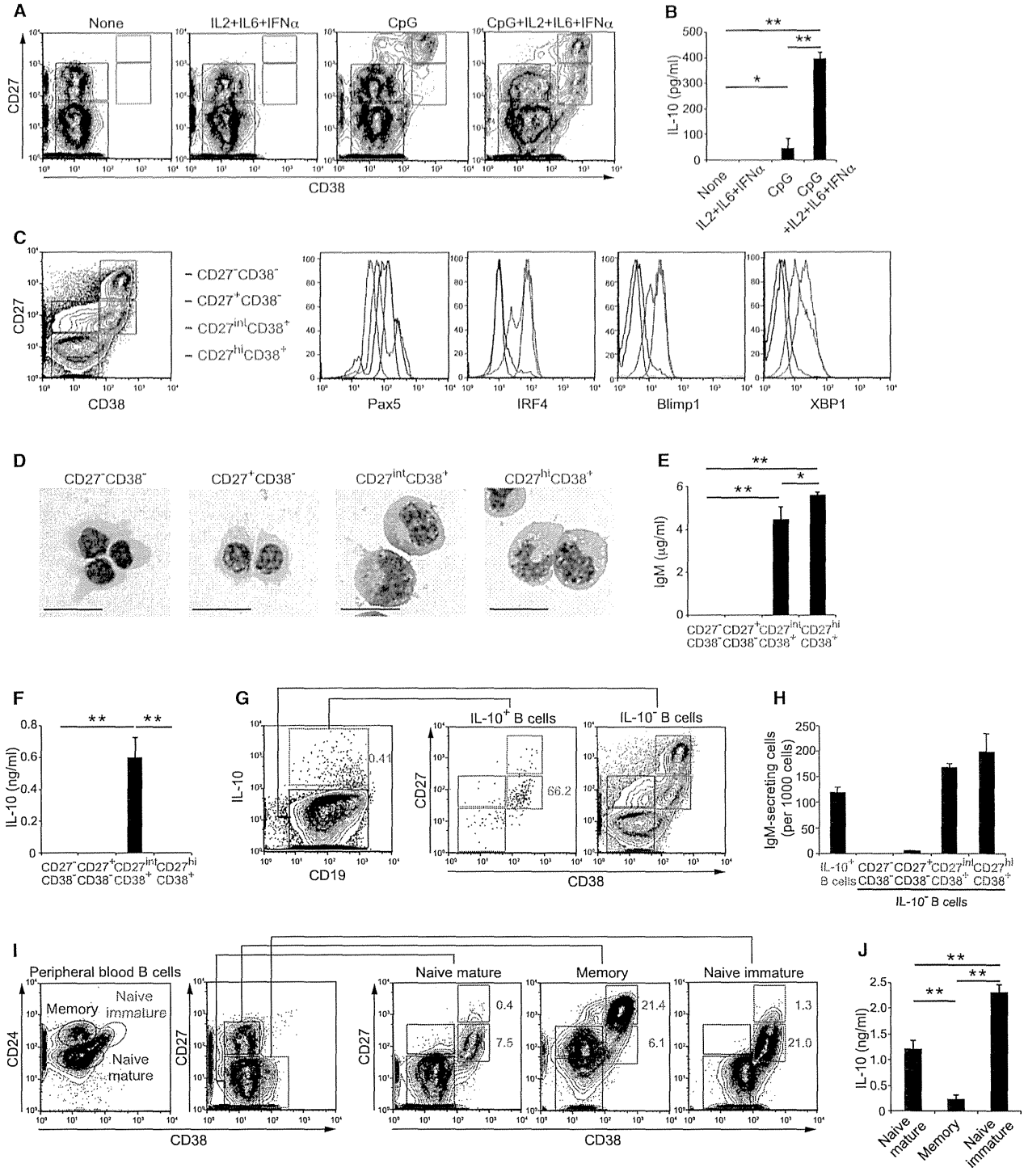

Figure 6. Human Plasmablasts Are IL-10-Producing B Cells

(A) Flow cytometry of B cells isolated from healthy blood donors and cultured with IL-2, IL-6 plus IFN-α (IL2, IL6, IFNα), and/or CpG for 96 hr. Four populations—$CD27^{-}CD38^{-}$ (red), $CD27^{+}CD38^{-}$ (blue), $CD27^{int}CD38^{+}$ (green), and $CD27^{hi}CD38^{+}$ (purple) cells—are gated.

(B) ELISA of IL-10 secreted by B cells isolated from peripheral blood of healthy donors and cultured with IL-2, IL-6 plus IFN-α, and/or CpG for 96 hr.

(C) Flow cytometry of B cell populations indicated in the left panel.

(legend continued on next page)

IRF4 binding to the same element in various types of cells (Cretney et al., 2011; Lee et al., 2009; Li et al., 2012). NFAT bound to the same region in Th2 cells, which was essential for IL-10 transcription (Lee et al., 2009). Taking into account our previous finding that B-cell-mediated IL-10 production requires NFAT activation (Matsumoto et al., 2011), it seems likely that IRF4 serves as an NFAT transcription partner to produce IL-10 in plasmablasts.

Unexpectedly, Blimp1-deficient B cells secreted IL-10 in our in vitro experiments despite impaired $CD138^+$ cell differentiation. Considering that the initiation of plasma cell differentiation takes place in vitro in the absence of Blimp1 (Kallies et al., 2007), it seems possible that IL-10 production is initiated already in the early preplasmablastic stage of plasma cell development, which is independent of Blimp1 (Kallies et al., 2007). However, we could detect little Venus-positive $CD138^-$ B cell population in mice during EAE (data not shown). Given that GFP^+CD138^- cells in *Prdm1*$^{gfp/+}$ mice were effectively generated in vitro (Figure 4A), but not in vivo (Figure 1B), it seems likely that no or few preplasmablasts as is detected in culture exist in vivo.

We now have evidence that naive B-cell-derived plasmablasts represent the most significant IL-10 producers in humans. Although activation of human peripheral blood B cells with CpG caused $CD27^{hi}CD38^+$ plasmablast generation, our results establish that additional treatment with cytokines including IL-2, IL-6, and, especially, IFN-α drove the differentiation of $CD27^{int}CD38^+$ plasmablasts that predominantly secrete IL-10. Given that IFN-α enhances $CD38^+$ expression on naive B cells (Giordani et al., 2009) and can induce plasma cell differentiation (Jego et al., 2003), IFN receptor signals seem likely to be key for IL-10-producing plasmablast generation. Indeed, patients with SLE have high serum IFN-α concentrations (Kim et al., 1987) and increased $CD27^{int}CD38^+$ cells in peripheral blood (Arce et al., 2001), suggesting that $IL\text{-}10^+$ plasmablast expansion might be the result of the inflammatory conditions. Furthermore, the treatment with IFN-β, another type I IFN approved for MS therapy, enhances B cell IL-10 secretion after BCR and CD40 ligation (Ramgolam et al., 2011). Although the precise mechanism by which IFN-β suppresses MS remains unclear, one of the possible explanations is that IFN-β might promote generation of IL-10-producing plasmablasts. Noteworthy, in clinical trials, MS patients who received Atacicept, a transmembrane activator and calcium-modulating cyclophilin-ligand interactor (TACI)-Ig fusion protein to deplete antibody-secreting cells, had exacerbated inflammatory symptoms (Hartung and Kieseier, 2010). This would be consistent with an inhibitory function for human plasmablasts. We have provided evidence that IL-10-producing plasmablasts effectively stem from naive immature B cells. This might support a recent study that human IL-10-competent B cells were enriched in immature $CD24^{hi}CD38^{hi}$ B cells after culture with CD40 stimulation (Blair et al., 2010). We found that memory B-cell-derived plasmablasts failed to secrete IL-10, suggesting that the immediate precursor of developing plasmablasts would dictate the balance between cells that promote autoimmunity by antibody production or have regulatory capacity that protects from overt pathology.

In conclusion, our findings have identified plasmablasts in the dLNs as the IL-10-producing B cells that suppress autoimmunity. We also established a phenotype for human plasmablasts that predominantly secreted IL-10. Our study might lead to better understanding of the nature of autoimmune diseases and provide a basis for exploring new therapeutic strategies.

EXPERIMENTAL PROCEDURES

Mice

C57BL/6 mice were purchased from CLEA Japan. *Bcl6*$^{yfp/yfp}$ (Kitano et al., 2011), *Il10*$^{Venus/+}$ (Atarashi et al., 2011), *Irf4*$^{-/-}$ (Mittrücker et al., 1997; Suzuki et al., 2004), *Mb1*$^{Cre/+}$ (Hobeika et al., 2006), μMT (Kitamura et al., 1991), and *Prdm1*$^{gfp/+}$ (Kallies et al., 2004) mice have been described previously. *Il10*$^{-/-}$, *Prdm1*$^{f/f}$, *Sell*$^{-/-}$, and TCR^{MOG} transgenic mice were purchased from the Jackson Laboratory. We generated *Prdm1*$^{f/f}$*Mb1*$^{Cre/+}$ mice by crossing of *Prdm1*$^{f/f}$ mice with *Mb1*$^{Cre/+}$ mice. Mice were bred and maintained under specific-pathogen-free conditions and used at 6 to 12 weeks of age. Animal care and experiments were conducted according to the guidelines established by the animal committee of Osaka University.

Generation of Mixed Bone Marrow Chimeras

Mixed bone marrow chimeras were produced as described previously (Fillatreau et al., 2002). In brief, recipient wild-type mice received 800 cGy of X-ray irradiation. One day later, the recipients were reconstituted with a mixed inoculum of 80% μMT bone marrow cells supplemented with 20% bone marrow cells from *Irf4*$^{-/-}$ or *Sell*$^{-/-}$ mice. Control groups received 80% μMT and 20% wild-type bone marrow cells or 80% wild-type and 20% bone marrow cells from *Irf4*$^{-/-}$ or *Sell*$^{-/-}$ mice. Chimeric mice were left to fully reconstitute their lymphoid system for at least 12 weeks before EAE induction.

Induction and Assessment of EAE

EAE was induced by subcutaneous immunization with 200 μg of MOG_{35-55} (MBL) emulsified in complete Freund's adjuvant (CFA) containing 500 μg of

(D) May-Grünwald-Giemsa staining of sorted B cell populations after culture with IL-2, IL-6, IFN-α plus CpG for 96 hr. Original magnification, ×400; scale bars represent 20 μm.

(E and F) ELISA of IgM (E) and IL-10 (F) secreted by the indicated B cell populations after culture with IL-2, IL-6, IFN-α plus CpG for 96 hr and then cultured for an additional 24 hr.

(G) Flow cytometry of B cells cultured with IL-2, IL-6, IFN-α plus CpG for 96 hr and labeled with IL-10 capture and detection antibodies to detect $IL\text{-}10^+$ B cells. Percentage of $IL\text{-}10^+$ B cells and $IL\text{-}10^+CD27^{int}CD38^+$ cells are shown.

(H) ELISPOT of IgM secreted by the indicated B cell populations after culture with IL-2, IL-6, IFN-α plus CpG for 96 hr followed by an additional 24 hr culture.

(I) Flow cytometry of three B cell populations freshly isolated from peripheral blood of healthy donors and then cultured with IL-2, IL-6, IFN-α plus CpG for 96 hr. Three major populations such as $CD24^{lo}CD27^-CD38^-$ (naive mature; red), $CD24^{hi}CD27^-CD38^{lo}$ (naive immature; pink), and $CD24^{hi}CD27^+CD38^-$ (memory; blue) cells in peripheral blood B cells before culture are gated (left two panels). Percentages of $CD27^{int}CD38^+$ and $CD27^{hi}CD38^+$ cells after culture are shown (right three panels).

(J) ELISA of IL-10 secreted by naive mature, naive immature, and memory B cells isolated from healthy blood donors and cultured with IL-2, IL-6, IFN-α plus CpG for 96 hr.

Data shown are representative of three independent experiments. See also Figure S6.

(B, E, F, H, and J) Data are presented as mean ± SD. *$p < 0.05$, **$p < 0.001$ (Student's t test).